Circulation Research
JOURNAL OF THE AMERICAN HEART ASSOCIATION

Synaptojanin-2 Binding Protein Stabilizes the Notch Ligands DLL1 and DLL4 and Inhibits Sprouting Angiogenesis

M. Gordian Adam, Caroline Berger, Anja Feldner, Wan-Jen Yang, Joycelyn Wüstehube-Lausch, Stefanie E. Herberich, Marcel Pinder, Sabine Gesierich, Hans-Peter Hammes, Hellmut G. Augustin and Andreas Fischer

Circ Res. 2013;113:1206-1218; originally published online September 11, 2013;
doi: 10.1161/CIRCRESAHA.113.301686
Circulation Research is published by the American Heart Association, 7272 Greenville Avenue, Dallas, TX 75231

Print ISSN: 0009-7330. Online ISSN: 1524-4571

Synaptojanin-2 Binding Protein Stabilizes the Notch Ligands DLL1 and DLL4 and Inhibits Sprouting Angiogenesis

M. Gordian Adam, Caroline Berger, Anja Feldner, Wan-Jen Yang, Joycelyn Wüstehube-Lausch, Stefanie E. Herberich, Marcel Pinder, Sabine Gesierich, Hans-Peter Hammes, Hellmut G. Augustin, Andreas Fischer

Rationale: **The formation of novel blood vessels is initiated by vascular endothelial growth factor. Subsequently, DLL4-Notch signaling controls the selection of tip cells, which guide new sprouts, and trailing stalk cells. Notch signaling in stalk cells is induced by DLL4 on the tip cells. Moreover, DLL4 and DLL1 are expressed in the stalk cell plexus to maintain Notch signaling. Notch loss-of-function causes formation of a hyperdense vascular network with disturbed blood flow.**

Objective: **This study was aimed at identifying novel modifiers of Notch signaling that interact with the intracellular domains of DLL1 and DLL4.**

Methods and Results: **Synaptojanin-2 binding protein (SYNJ2BP, also known as ARIP2) interacted with the PDZ binding motif of DLL1 and DLL4, but not with the Notch ligand Jagged-1. SYNJ2BP was preferentially expressed in stalk cells, enhanced DLL1 and DLL4 protein stability, and promoted Notch signaling in endothelial cells. SYNJ2BP induced expression of the Notch target genes HEY1, lunatic fringe (LFNG), and ephrin-B2, reduced phosphorylation of ERK1/2, and decreased expression of the angiogenic factor vascular endothelial growth factor (VEGF)-C. It inhibited the expression of genes enriched in tip cells, such as angiopoietin-2, ESM1, and Apelin, and impaired tip cell formation. SYNJ2BP inhibited endothelial cell migration, proliferation, and VEGF-induced angiogenesis. This could be rescued by blockade of Notch signaling or application of angiopoietin-2. SYNJ2BP-silenced human endothelial cells formed a functional vascular network in immunocompromised mice with significantly increased vascular density.**

Conclusions: **These data identify SYNJ2BP as a novel inhibitor of tip cell formation, executing its functions predominately by promoting Delta-Notch signaling. (*Circ Res*. 2013;113:1206-1218.)**

Key Words: angiogenesis ■ blood vessels ■ DLL4 ■ endothelial cell differentiation ■ Notch ■ SYNJ2BP

Angiogenesis, the formation of novel blood vessels from preexisting vessels, is essential for embryonic development as well as for tissue growth and wound healing in the adult.[1] Excessive angiogenesis is frequently observed in solid tumors and in some hematological malignancies. For instance, increased blood vessel densities have been detected in the bone marrow of patients with leukemia or myeloma. Consistently, angiogenesis inhibitors show some clinical efficiency.[2] Uncontrolled angiogenesis also underlies choroidal neovascularization, which leads to vision threatening (wet macular degeneration)[3] and might be causative for the formation of vascular malformations.[4] Antiangiogenic drugs have been approved for treatment of several tumor entities and wet macular degeneration. Although blocking vascular endothelial growth factor (VEGF) in the eye is highly efficient,[3] most malignant tumors become resistant to anti-VEGF therapy.[1] Thus, targeting of additional angiogenic factors will be necessary for future therapy.

Editorial see p 1186
In This Issue, see p 1181

Angiogenic sprouting is initiated in response to stimulatory cues like VEGF, which destabilize cellular contacts, promote degradation of the extracellular matrix, and stimulate quiescent endothelial cells to become migratory and invasive.[5] It is essential that only few endothelial cells respond to the growth stimuli and subsequently guide the formation of new capillary sprouts as tip cells. This selection process between tip cells and the trailing stalk cells, which are less motile but form the lumen of

Original received April 29, 2013; accepted September 11, 2013. In August 2013, the average time from submission to first decision for all original research papers submitted to *Circulation Research* was 12.8 days.

From Division of Vascular Signaling and Cancer (M.G.A., C.B., A.F., W.-J.Y., S.E.H., A.F.) and Division of Vascular Oncology and Metastasis (S.G., H.G.A.), German Cancer Research Center (DKFZ-ZMBH Alliance), Heidelberg, Germany; Division of Vascular Biology and Tumor Angiogenesis (M.G.A., C.B., W.-J.Y., J.W.-L., S.E.H., M.P., H.G.A., A.F.) and Fifth Medical Department (H.-P.H.), Medical Faculty Mannheim, Heidelberg University, Mannheim, Germany; and BioNTech AG, Mainz, Germany (J.W.-L.).

The online-only Data Supplement is available with this article at http://circres.ahajournals.org/lookup/suppl/doi:10.1161/CIRCRESAHA.113.301686/-/DC1.

Correspondence to Andreas Fischer, Division of Vascular Signaling and Cancer (A270), German Cancer Research Center (DKFZ-ZMBH Alliance), Im Neuenheimer Feld 280, 69120 Heidelberg, Germany. Email a.fischer@dkfz-heidelberg.de

Nonstandard Abbreviations and Acronyms	
GFP	green fluorescent protein
HUAEC	human umbilical artery endothelial cell
HUVEC	human umbilical vein endothelial cell
NICD	intracellular Notch domain
SYNJ2BP	synaptojanin-2 binding protein

the new vessel, is predominantly regulated by Notch signaling. Tip cells are characterized by extensive filopodia, which express high levels of VEGF receptor-2 and VEGF receptor-3 and act as sensors of the VEGF gradient.[6] VEGF induces the expression of the Notch ligand DLL4 in tip cells. The transmembrane DLL4 protein binds to Notch1 receptors in the adjacent stalk cells, leading to cleavage and release of the intracellular Notch domain (NICD). NICD translocates to the nucleus and acts as a transcriptional regulator controlling the expression of multiple cell type–specific genes. The induction of common target genes of the HES or HEY transcription factor families is generally observed in many different cell types and is considered an indicator of Notch activity.[7] HEY and HES proteins repress the expression of VEGF receptors, thus rendering stalk cells and endothelial cells of mature vessels less responsive to VEGF.[8] Consistently, inhibition of Notch by genetic or pharmacological approaches leads to higher tip cell numbers with increased angiogenic sprouting and branching, whereas Notch gain-of-function inhibits vessel branching.[9–11] Interestingly, Notch signals are also required in vessels of the adult to maintain the quiescent endothelial phenotype. Long-term deletion of DLL4-Notch signaling in the adult may consequently result in the formation of vascular tumors[12,13] or vascular malformations.[4]

It is important to note that tip cells and stalk cells change their positions and thus change their cellular functions during angiogenesis.[14] This appears to be guided by oscillatory gene expression loops of Notch, BMP, and probably additional signaling pathways. These oscillations determine time periods in which cells are responsive for tip or stalk cell–promoting factors.[15,16] Second, the expression of Notch ligands in tip and stalk cells is not a simple black-and-white situation. Although tip cells express high amounts of DLL4, this protein was also detected in stalk cells, capillaries, and arterioles, although at lower levels.[9,17] Moreover, the related Notch ligand DLL1 is expressed in the stalk cells and is absent from tip cells.[17] Consistently, Notch activity was observed throughout the stalk cell plexus in Notch reporter mice.[9,17] This indicates that Notch receptors on stalk cells are activated not only by ligand-expressing tip cells but also by ligands on adjacent stalk cells. This is supported by genetic loss-of-function experiments of either Notch1 or DLL4, which demonstrated tip cell formation and excessive branching within the stalk cell plexus[8–11] and subsequent defects in vascular remodeling.[18]

The present study was aimed at identifying novel regulators of Delta-Notch signaling during angiogenesis. Among the most promising candidate molecules, a yeast 2-hybrid screen identified Synaptojanin-2 binding protein (SYNJ2BP, also known as ARIP2 or OMP25) as a novel intracellular interaction partner of DLL1 and DLL4. SYNJ2BP is a small protein (145 amino acids) containing a single PDZ domain. PDZ domain proteins often act as scaffolds and modify the function, stabilization, or localization of transmembrane proteins. SYNJ2BP regulates the localization of Synaptojanin-2 and the endocytosis of activin type II receptors.[19,20] This PDZ protein is widely expressed in mouse and rat tissues[20,21] and may play a role in cancer progression.[22] We hypothesized that SYNJ2BP may act as an important regulator in the control of Delta-Notch signaling during angiogenesis and, consequently, we pursued a systematic study of SYNJ2BP function in the regulation of angiogenic endothelial cell functions.

Methods

An expanded Methods section is available in the Online Data Supplement.

Endothelial Migration, Proliferation, Adhesion, Tube Formation, and Sprouting

Analyses of human umbilical vein endothelial cell (HUVEC) migration, proliferation, and spheroid sprouting in collagen beds of siRNA-transfected or viral-transduced HUVECs were performed as described.[23]

Cycloheximide Assay/DLL1 and DLL4 Half-Life Determination

To assess protein stability, human umbilical artery endothelial cells (HUAECs) were transduced with green fluorescent protein (GFP) or SYNJ2BP adenovirus. After 48 hours, the growth medium was replaced with medium containing 0.1 mmol/L cycloheximide to halt protein biosynthesis. Cells were treated for 0 to 8 hours and then harvested for Western blotting.

In Vivo Spheroid-Based Angiogenesis Assay

The in vivo spheroid-based angiogenesis assay was performed as described[24,25] with spheroids from pooled HUVECs injected subcutaneously into the flank of 6-week-old to 8-week-old female CB17 severe combined immunodeficiency mice (Charles River). Plugs were removed after 28 days and fixed in 4% formaldehyde before embedding in paraffin. Sections (5 μm) were stained with antihuman CD34 (QBEND10; Menarini Diagostics) and anti-α-smooth muscle actin-Cy3 (Sigma-Aldrich).

Quantitative Reverse-Transcription Polymerase Chain Reaction

Total RNA was isolated using the RNeasy Kit (Qiagen), and 2 μg RNA was transcribed into cDNA using the SuperScript II reverse transcriptase and random hexamer primers (Invitrogen). Quantitative polymerase chain reaction was performed with the POWER SYBR Green Master Mix on an ABI StepOnePlus cycler. All polymerase chain reaction primer sequences are listed in Online Table I.

Statistical Analysis

Results are expressed as means±SD. Comparisons between groups were analyzed by *t* test (2-sided). Degradation rates were analyzed with a 2-way ANOVA. $P<0.05$ were considered significant.

Results

DLL4 Physically Interacts With SYNJ2BP, MUPP1, and MAGI Proteins

Yeast 2-hybrid screening using the intracellular domain of DLL4 as bait and an embryonic cDNA library as prey identified SYNJ2BP, MUPP1, MAGI2, and MAGI3 as novel putative binding proteins of DLL4. The same interacting proteins were also retrieved in a screen using the intracellular domain of DLL1 as bait (Figure 1A). MAGI1 was also isolated but showed characteristics of a typical false-positive clone in subsequent

A Yeast two-hybrid

	MAGI2	MAGI3	MUPP1	SYNJ2BP	DLL1	DLL4
DLL1ic	+	+	+	+	-	-
DLL1ic-ΔPDZ	-	-	-	-	-	-
DLL4ic	+	+	+	+	-	-
DLL4ic-ΔPDZ	-	-	-	-	-	-
JAG1ic	n.d.	n.d.	-	-	n.d.	n.d.

B *in silico* analysis

	DLL1	DLL4	JAG1
SYNJ2BP	+++ 1,08 (<1.2%)	+++ 1,08 (<1.2%)	+/- 0,59 (<17%)
MAGI1 (PDZ#3)	+++ 1,02 (<1.3%)	+++ 1,02 (<1.3%)	- 0,45 (<33%)
MAGI2 (PDZ#2)	+++ 1,12 (<1%)	+++ 1,12 (<1%)	+ 0,73 (<7%)
MAGI3 (PDZ#1)	+++ 1,01 (<1%)	+++ 1,01 (<1%)	+/- 0,64 (<12%)
MUPP1 (PDZ#13)	+++ 0,96 (<2%)	+++ 0,96 (<2%)	+/- 0,54 (<17%)

C interaction in HEK293

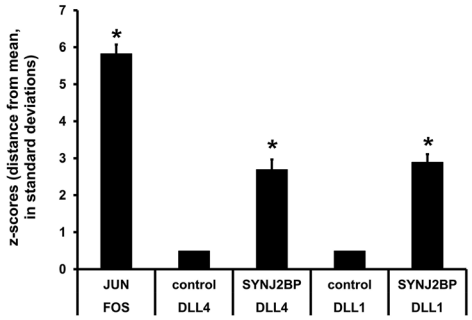

D interaction in HUVEC

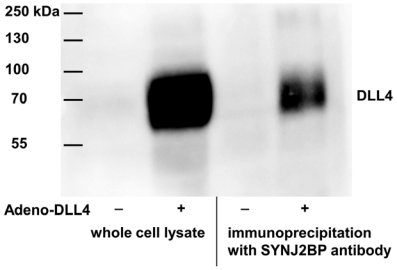

Figure 1. Synaptojanin-2 binding protein (SYNJ2BP) interacts with Notch ligands. A, A yeast 2-hybrid screening identified SYNJ2BP, MAGI2, MAGI3, and MUPP1 as interaction partners of the intracellular DLL1 and DLL4 domains (ic). Protein interactions were further tested by mating AH109 yeast carrying pGBK plasmid encoding Notch ligand contructs with the Y187 yeast strain harboring pGAD plasmids encoding the PDZ proteins. DLL1 and DLL4 lacking the PDZ peptide did not bind to these proteins, suggesting a direct PDZ domain–PDZ peptide binding. n.d. indicates not determined. **B**, In silico analyses predicted binding of the respective PDZ domains to PDZ sequences (IATEV) of DLL1 and DLL4 and Jagged-1 (MEYIV). The use of the prediction matrix resulted in the numeric value ψ associated with the binding probability. The chance for a false-positive correlation is given in parentheses. The binding likelihood is shown with + and –. **C**, A LUMIER interaction assay showed binding of protein A–tagged SYNJ2BP to luciferase-tagged DLL1 and DLL4 in HEK293 cells after coimmunoprecipitation. The strong interaction of JUN and FOS served as a positive control. As negative controls, luciferase-tagged DLL1 and DLL4 were incubated with protein A only. n=3; **P*<0.05. **D**, Human umbilical vein endothelial cells were transduced with SYNJ2BP and DLL4. Interaction of the proteins was demonstrated by detection of DLL4 after immunoprecipitation of SYNJ2BP.

analyses in yeast. This is relevant insofar as MAGI1 and MAGI2 (Acvrinp1) have previously been reported to bind DLL1.[26,27] All identified proteins contain PDZ domains and thus should bind to the carboxyterminal PDZ binding motif (amino acids IATEV) of DLL1 and DLL4. In silico analyses using a statistical model that predicts PDZ domain–peptide interactions[28] supported this hypothesis and predicted a high probability for interactions of MAGI2, MAGI3, MUPP1, and SYNJ2BP with DLL1 and DLL4 (Figure 1B). This algorithm predicted much lower interaction probabilities for putative binding of the Notch ligand Jagged-1 (JAG1), which harbors a different PDZ binding motif (amino acids MEYIV; Figure 1B). Yeast 2-hybrid experiments showed no binding of JAG1 to SYNJ2BP (Figure 1A). The PDZ domain/PDZ binding motif interactions were verified in yeast cells in which the intracellular domains of DLL1 and DLL4, but not those lacking the terminal 4 amino acids ATEV, bound to MAGI2, MAGI3, MUPP1, and SYNJ2BP (Figure 1A). The interaction of SYNJ2BP with DLL1 and DLL4 was also observed in transiently transfected human HEK293 cells. Full-length human proteins were tagged with protein A or luciferase and the interactions between SYNJ2BP and Delta ligands were detected by bioluminescence after coimmunoprecipitation (LUMIER assay[29]; Figure 1C). Moreover, DLL4 and SYNJ2BP could be coprecipitated in HUVECs when overexpressed (Figure 1D). Based on this, we decided to analyze the impact of SYNJ2BP on Delta-Notch signaling in endothelial cells.

SYNJ2BP Partially Overlaps With DLL4 Expression

Primary human endothelial cells of venous (HUVEC) and arterial origin (HUAEC) expressed similar amounts of SYNJ2BP (Online Figure I). SYNJ2BP protein expression was observed in intracellular vesicles and also at the cell membrane, and partially colocalized with DLL4, when overexpressed (Figure 2A). Endogenous SYNJ2BP protein could also be detected in murine primary lung endothelial cells (Online Figure IIA and IIB). In mouse embryos, SYNJ2BP protein was ubiquitously expressed with especially strong expression in the neural tube and in blood vessels of venous and arterial origin (Figure 2B). SYNJ2BP expression was much more abundant compared with DLL4, the expression of which is more restricted to the arterial lineage. In line with this, SYNJ2BP and DLL4 only partially colocalized in the postnatal retinal vasculature of mice. This vascular bed developed after birth in a stereotypical manner. SYNJ2BP was expressed in arterial and venous beds with highest levels in stalk cells (Figure 2C). It is well-known that Delta ligand expression is not only restricted to tip cells. DLL4 is the only Notch ligand in tip cells, but together with DLL1 it may also be present in stalk cells at lower levels, where it overlaps with SYNJ2BP expression (Figure 2D). DLL1 is expressed in stalk cells, arteries, and veins of the developing retina[9,17]; this also overlaps with SYNJ2BP expression.

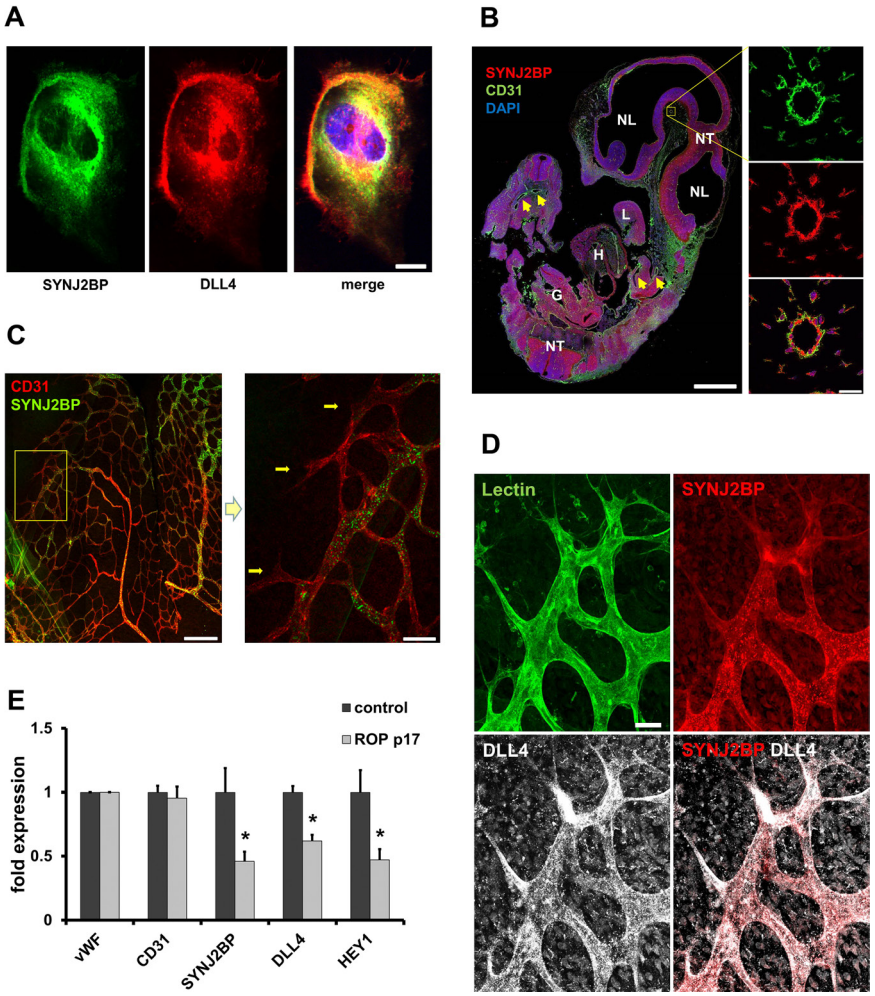

Figure 2. Synaptojanin-2 binding protein (SYNJ2BP) colocalizes with DLL4. A, Human umbilical vein endothelial cells were transduced with SYNJ2BP and DLL4 and stained for both proteins after 48 h. Representative images are shown. DLL4 (Alexa546; red) and SYNJ2BP (Alexa488; green) colocalized at the cell membrane and within cytoplasmic vesicles. Scale bar, 10 μm. **B**, C57BL/6 murine embryonic day (E) 11.5 embryos were stained for CD31 (Alexa488; green) and SYNJ2BP (Cy3; red). Scale bar, 500 μm. G indicates gut; H, heart; L, limb; NL, neural lumen; and NT, neural tube. Arrows denote dorsal aorta and cardinal vein. A blood vessel from the head was enlarged to demonstrate the high abundance of SYNJ2BP in the vasculature. Scale bar, 20 μm. **C**, Retinae from C57BL/6 mice (p5) were stained for CD31 (Cy3; red) to visualize the vasculature. Costaining for SYNJ2BP (Alexa488; green) revealed that the protein expression is restricted to the vasculature and most abundant in the stalk cell plexus. Scale bar, 200 μm. The magnification revealed that SYNJ2BP is mostly absent from tip cells (arrows). Scale bar, 50 μm. **D**, High-magnification image of the leading edge in a developing retinal vasculature in C57BL/6 mice (p5). Blood vessels were visualized with lectin (FITC; green). Staining for Dll4 (Cy5; white) confirmed that the protein is present in both tip and stalk cells with higher amount in tip cells. Costaining for SYNJ2BP (Cy3; red) revealed colocalization with DLL4 in stalk cells. Scale bar, 20 μm. All images were taken with a Zeiss LSM 700 confocal microscope. **E**, Retinae were taken from wild-type mice (p17) subjected to hyperoxia/normoxia to induce pathologically increased angiogenesis (retinopathy of prematurity, ROP). Quantitative polymerase chain reaction showed decreased expression levels of DLL4 and the primary Notch target gene HEY1. Also, SYNJ2BP expression was decreased compared with untreated littermates. Results are expressed as means±SD. n=3; **P*<0.05.

Finally we determined quantitative expression of SYNJ2BP and DLL4 in retinal endothelial cells undergoing hypoxia-induced angiogenesis. Newborn mice at postnatal day 7 were exposed to hyperoxia (75% oxygen) for 5 days and then returned to room air. This procedure causes vasoregression of retinal vessels, followed by excessive outgrowth of immature vessels. Thus, this experiment mimics retinopathy of prematurity. The retinae were harvested at day 17, that is, during the angiogenic period.[30] Quantitative polymerase chain reaction was performed with normalization to CD31 and von Willebrand factor mRNA, which are rather exclusively expressed in endothelial cells. This revealed that expressions of SYNJ2BP, DLL4, and the Notch target gene HEY1 were significantly decreased in this immature vasculature (Figure 2E). This is consistent with the findings that decreased Notch activity causes excessive angiogenic sprouting of immature vessels and that SYNJ2BP may be involved in the control of angiogenesis.

SYNJ2BP Inhibits Blood Vessel Formation In Vivo

Because of the lack of a suitable knockout mouse model (because the BayGenomics gene trap ES cell line RRB066 did not produce a null allele), we used an established xenografting assay to determine the role of SYNJ2BP in vivo. This assay allows the generation of a human vasculature in mice by subcutaneous implantation of genetically modified HUVEC

spheroids.[4,23–25] HUVECs were lentivirally infected with shRNA targeting SYNJ2BP, causing a stable knockdown of SYNJ2BP expression to ≈30% (Online Figure IIC). HUVEC spheroids were transplanted in a growth factor–rich Matrigel and fibrin matrix into severe combined immunodeficiency mice. The grafted human endothelial cells formed blood vessels, which anastomozed with the mouse vasculature. This enabled perfusion of the human vessels and recruitment of mural cells (Figure 3). The plugs were resected 4 weeks after grafting and were analyzed by immunohistochemistry. The perfusion rate and coverage with α-smooth muscle actin–positive mural cells were not altered between the 2 groups (Figure 3A–D). However, the microvascular density was significantly higher in the plugs grafted with SYNJ2BP-silenced HUVECs compared with such expressing control shRNA (Figure 3A, 3B, and 3E). Thus, SYNJ2BP acted as an antiangiogenic molecule in vivo.

Second, we analyzed how forced expression of SYNJ2BP affects the outgrowth of capillary sprouts from segments of the mouse aorta. Aortic rings were adenovirally infected with SYNJ2BP or GFP cDNA and embedded in Matrigel. VEGF induced the outgrowth of capillary-like structures under control conditions, and these cells expressed the endothelial cell marker CD31. However, enforced SYNJ2BP expression abolished angiogenesis from aortic rings (Figure 3F and 3G). This again indicates that SYNJ2BP acts as an antiangiogenic protein.

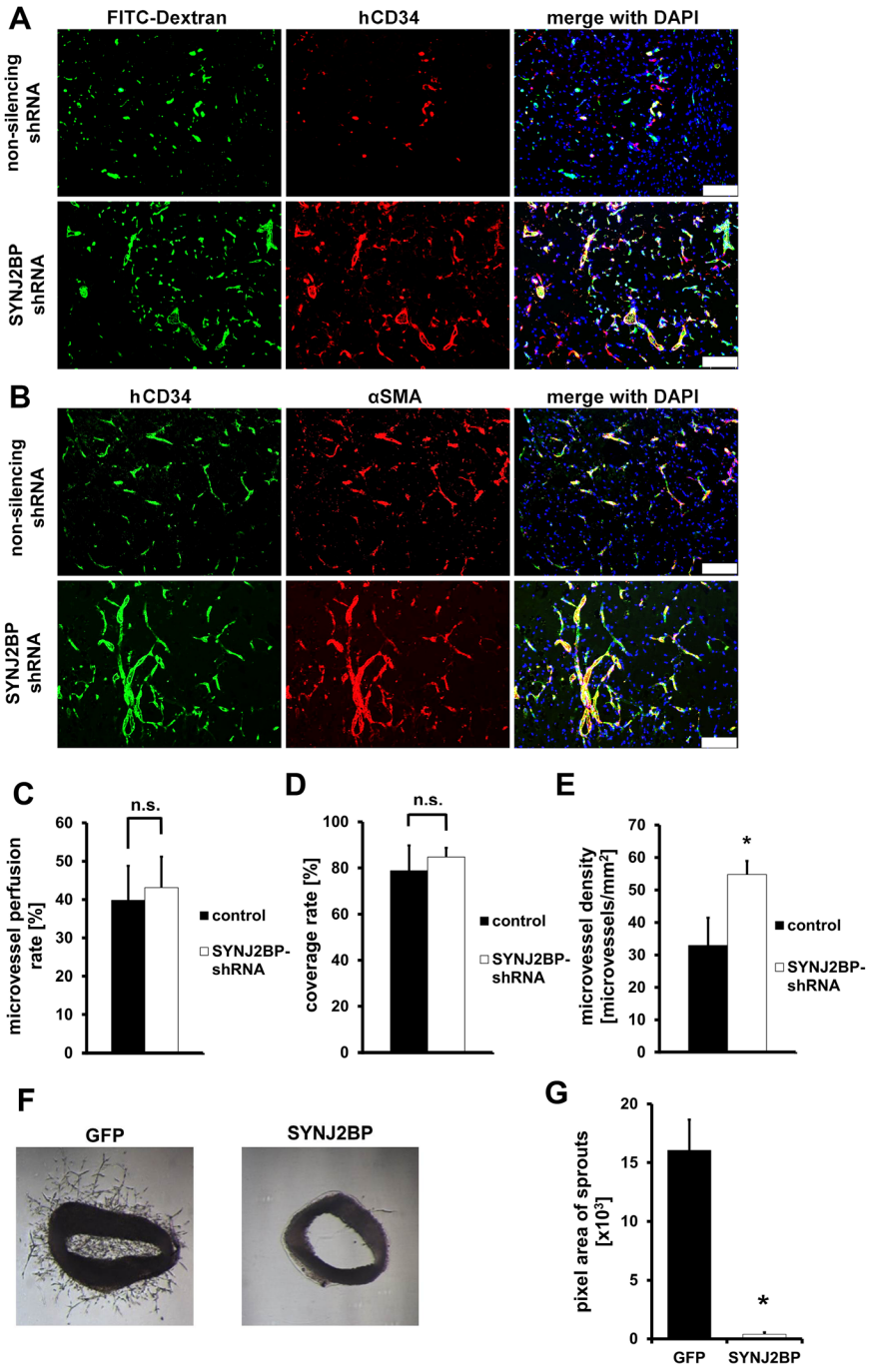

Figure 3. Synaptojanin-2 binding protein (SYNJ2BP) acts as an antiangiogenic protein in vivo. Human umbilical vein endothelial cells (HUVECs) were lentivirally infected with shRNA against SYNJ2BP and injected as spheroids in a Matrigel/fibrin matrix into nude mice. The plugs were analyzed after 28 days. Fifty percent of the animals were intravenously injected with FITC-dextran to determine perfusion of the neovasculature. **A**, Representative images of the neovasculature. Vessels of HUVEC origin were stained with human-specific CD34 (Cy3; red); perfused vessels were labeled with FITC-dextran (green). Nuclei were stained with DAPI (blue). **B**, Microvessel density (human CD34; Alexa488; green) and coverage with α-smooth muscle actin (αSMA)-positive mural cells (Cy3; red). Images were taken with an Axiovision Z1 fluorescence microscope (Zeiss) at 10-fold magnification. Contrast was enhanced with Axiovision Rel. 4.7 software. Scale bars, 100 μm. **C**, Quantification of the blood vessel perfusion rate showed no significant difference between SYNJ2BP-silenced and control vessels. **D**, Endothelial coverage with αSMA-positive mural cells was not affected by SYNJ2BP silencing in the endothelial cells. **E**, Quantification of the microvessel density per mm^2. SYNJ2BP-silenced human endothelial cells formed a significantly denser vessel network compared with control. n=4 plugs for SYNJ2BP shRNA; n=5 plugs for nonsilencing shRNA. At least 6 complete sections were analyzed per plug (≈200–250 images). Results are expressed as means±SD. *P<0.05. **F**, Representative pictures of aortic rings from wild-type mice treated with SYNJ2BP or green fluorescent protein adenovirus as a control. **G**, Quantification of the aortic ring sprouting activity of 18 rings from 3 mice. Results are expressed as means±SE. *P<0.05.

SYNJ2BP Expression Inhibits Sprouting Angiogenesis

We have previously shown that DLL4-Notch loss-of-function enhances sprouting angiogenesis, whereas gain-of-function prevents growth factor–induced sprouting, proliferation, and migration of endothelial cells.[23] Forced SYNJ2BP expression (Online Figure IID and IIE) phenocopied the functions of Notch and blocked VEGF-induced or FGF2-induced sprouting (Figure 4A and 4B). Silencing of SYNJ2BP by siRNA duplexes caused increased angiogenesis even under basal conditions (Figure 4C and 4D). This increase of the cumulative sprout length because of increased length of individual sprouts and because of higher sprout numbers (Online Figure III). The observed SYNJ2BP functions are in line with the known roles of DLL4-Notch signaling as a negative regulator of tip cell formation and endothelial cell proliferation.

SYNJ2BP Restricts Endothelial Proliferation and Migration

Angiogenesis is dependent on several cellular processes, including endothelial cell migration, proliferation, and adhesion. Migration of HUVECs during closure of a gap within an endothelial monolayer was significantly reduced by SYNJ2BP overexpression and enhanced after silencing of SYNJ2BP expression (Figure 5A and 5B; Online Figure IVA and IVB). This was not because of altered endothelial cell adhesion because SYNJ2BP had no effects on adhesion of HUVECs to the extracellular matrix components collagen or fibronectin (Online Figure IVC).

The phosphorylation of AKT/protein kinase B involved in cell survival signaling was not altered by SYNJ2BP (Online Figure IVD), and the apoptosis rate was not changed. However, proliferation of HUVECs was impaired by SYNJ2BP expression and enhanced after siRNA-mediated silencing of SYNJ2BP expression (Figure 5C and 5D). Consistently, SYNJ2BP had a negative effect on MAPK signaling as indicated by decreased phosphorylation of ERK proteins (Figure 5E). This again was reminiscent of established NOTCH1 functions in endothelial cells.[1,8,9,23]

SYNJ2BP Promotes Notch Signaling

The experiments described so far indicate that SYNJ2BP executes antiangiogenic functions in vitro and in vivo. The protein interactions with DLL4 and activin type II receptors imply that these signaling pathways are responsible for the observed functions. We analyzed whether SYNJ2BP gain-of-function or loss-of-function (Online Figure II) in HUVECs could influence Notch and activin signaling. SYNJ2BP expression attenuated activin-mediated phosphorylation of SMAD2/3, supporting the notion that SYNJ2BP inhibits activin signaling.[19,31] However, activin was described as an inhibitor of sprouting angiogenesis,[32] and our data support this (Figure 6A and 6B). Therefore, inhibition of activin signaling cannot explain the antiangiogenic roles of SYNJ2BP.

Forced lentiviral SYNJ2BP expression led to increased transcription of the primary Notch target genes HEY1 and LFNG, indicating increased Notch activity (Figure 6C). This could be verified in a Western blot showing increased levels of activated Notch (NICD) protein after forced expression of SYNJ2BP (Figure 6D). The glycosyltranferase LFNG modifies Notch receptors and thereby enhances DLL4-Notch signaling during angiogenesis.[33] Furthermore, expression of ephrin-B2 was induced. Consistently, lentiviral silencing of SYNJ2BP with 2 independent shRNA constructs (Online Figure IIC) decreased Notch activity and ephrin-B2 expression (Figure 6C). Ephrin-B2 is crucial for VEGF receptor trafficking, arterial fate differentiation, and tip/stalk cell selection during sprouting angiogenesis.[34,35] To test whether SYNJ2BP regulates HEY1, LFNG,

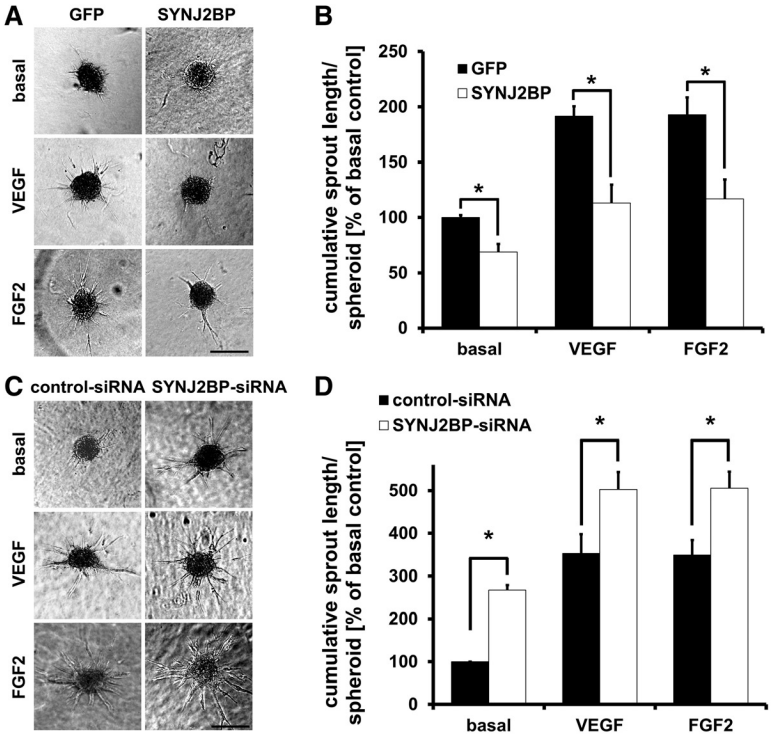

Figure 4. Synaptojanin-2 binding protein (SYNJ2BP) regulates sprouting angiogenesis. **A**, Representative images of human umbilical vein endothelial cell (HUVEC) spheroids infected with adenovirus to express SYNJ2BP or green fluorescent protein (GFP). Images were taken with a phase-contrast microscope (Olympus IX50) at 10-fold magnification. Scale bar, 100 μm. **B**, SYNJ2BP expression caused significantly decreased sprouting angiogenesis. Analysis was performed with the cell^p software. n=4 independent assays, 10 spheroids per assay. **C**, HUVEC spheroids transfected with SYNJ2BP siRNA or control siRNA with and without stimulation with 25 ng/mL FGF2 or vascular endothelial growth factor (VEGF). Scale bar, 100 μm. **D**, SYNJ2BP silencing showed significantly increased cumulative sprouting. n=4 independent assays, 10 spheroids per assay. Results are expressed as means±standard deviation. *P<0.05.

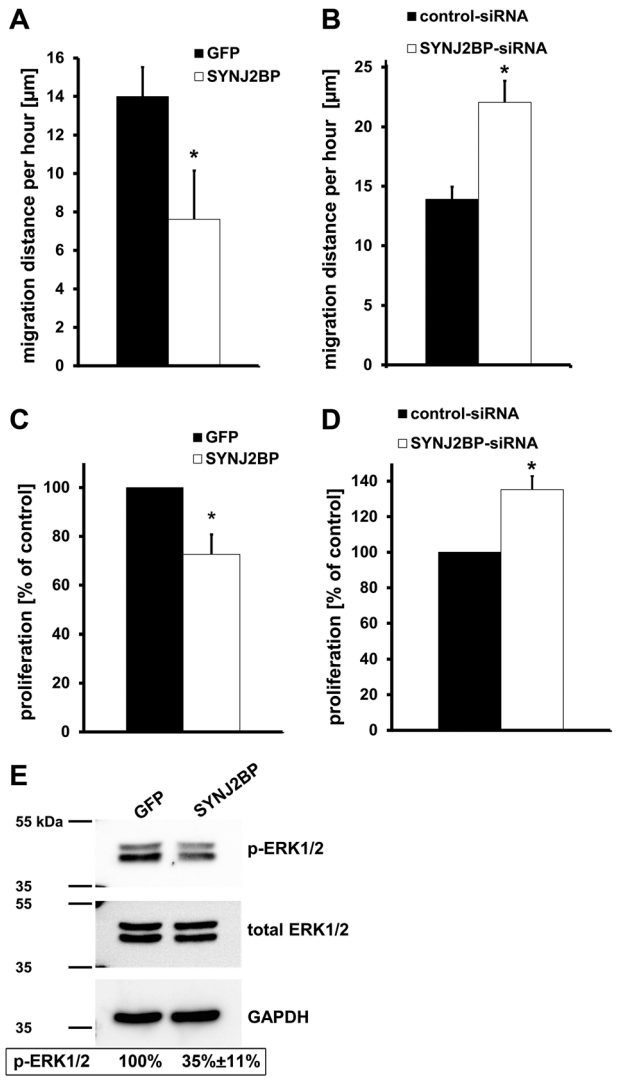

Figure 5. Synaptojanin-2 binding protein (SYNJ2BP) expression controls endothelial migration and proliferation. A, Adenoviral SYNJ2BP expression led to decreased human umbilical vein endothelial cell (HUVEC) migration in a wound-healing assay compared with green fluorescent protein–expressing cells. n=4 independent assays, 4 wells each. **B**, SYNJ2BP silencing resulted in a significantly increased endothelial migration. n=4 independent assays, 4 wells each. **C**, Forced expression of SYNJ2BP led to decreased bromodeoxyuridine incorporation in HUVECs, indicating less proliferation. n=5 independent assays, 5 wells each. **D**, HUVEC proliferation was increased after SYNJ2BP silencing compared with control siRNA-treated cells. n=5 independent assays, 5 wells each. **E**, Western blot analysis showed that phosphorylation of ERK1/2 was significantly decreased to 35% after 48 h of adenoviral SYNJ2BP infection. Expression was normalized to GAPDH. n=4 independent experiments. Results are expressed as means±SD. *P<0.05.

and ephrin-B2 directly through Notch signaling, HUVECs were transduced with SYNJ2BP-expressing lentivirus and the γ-secretase inhibitor N-[(3,5-difluorophenyl)acetyl]-L-alanyl-2-phenyl]glycine-1,1-dimethylethylester (DAPT) was added after 24 hours to block Notch receptor cleavage. This normalized gene expression levels of LFNG and HEY1 strongly reduced ephrin-B2 mRNA levels (Figure 6E). Furthermore, we observed that constitutively active constructs of NOTCH1 (ca-NICD) or its transducer RBPJκ (ca-RBPSUH-VP16) induced ephrin-B2 expression, whereas blockade of canonical Notch signaling with dominant-negative Mastermind-like 1 reduced ephrin-B2 mRNA levels (Figure 6F). These results correspond to previous observations that ephrin-B2 is a direct Notch target gene in endothelial cells.[36] Taken together, SYNJ2BP expression in endothelial cells induced Notch signaling, which is known to promote the stalk cell phenotype.[1,8,9]

Next, we determined the mRNA levels of several other known factors regulating endothelial guidance and tip/stalk cell formation. VEGF-A, SLIT1, SLIT2, ROBO1, ROBO4, Semaphorin-3A, Neuropilin-1, and Neuropilin-2 expression levels were not altered by SYNJ2BP. However, mRNA amounts of the pro-angiogenic factor VEGF-C and the tip cell–enriched genes[37] angiopoietin-2 (ANGPT2), ESM1, and Apelin were reduced by SYNJ2BP overexpression and increased after SYNJ2BP silencing (Figure 6G). The expressions of ESM1 and Apelin were dependent on Notch signaling, whereas ANGPT2 and VEGF-C were not (Figure 6H). Thus, SYNJ2BP regulates several crucial factors guiding angiogenesis. The majority occurs in a Notch-dependent manner, whereas ANGPT2 and VEGF-C are at least not directly affected by Notch signaling.

SYNJ2BP Promotes the Stalk Cell Phenotype

Notch signaling is intimately linked to the selection of tip and stalk cells, and ANGPT2 expression is highly enriched in tip cells.[37,38] To analyze tip cell behavior, we mixed HUVECs labeled with GFP or a red fluorescent dye in a 1:1 ratio before spheroid formation and embedded them in a collagen matrix. The probability of detecting a red or green endothelial cell at the growing tip was ≈50%. However, if SYNJ2BP expression was increased by viral transduction 48 hours before, then the SYNJ2BP-expressing HUVECs acquired the tip position significantly less frequently, whereas SYNJ2BP-silenced cells were found at the tip position at much higher rates (Figure 7A and 7B). Thus, SYNJ2BP expression not only inhibits expression of tip cell–enriched genes like ANGPT2, Apelin, and ESM1 (Figure 6G) but also limits the probability of acquiring the tip cell position. This fits well with the observed expression pattern of SYNJ2BP protein, which was predominantly found in stalk cells of the murine retina (Figure 2C and 2D).

Antiangiogenic Functions of SYNJ2BP Are Predominantly Mediated by Notch and ANGPT2 Signaling

To test the functional significance of these deregulated genes, we applied recombinant VEGF-C, ANGPT2, or Notch inhibitors to endothelial cells overexpressing SYNJ2BP. Recombinant VEGF-C and VEGF-A could not rescue sprouting angiogenesis (Figure 4A and Figure 7C). However, the application of recombinant ANGPT2 in combination with VEGF-A was sufficient to restore sprouting capacity (Figure 7D and 7E).

Finally, SYNJ2BP-expressing HUVEC spheroids were treated with the Notch inhibitor DAPT or the solvent DMSO as control. SYNJ2BP strongly inhibited VEGF-induced sprouting angiogenesis, but the γ-secretase inhibitor DAPT fully restored the angiogenic potential (Figure 7F and 7G). The reciprocal relationship between SYNJ2BP and Notch activity could also be shown in a complementary experiment in which the expression of active NOTCH1 (NICD) normalized endothelial sprouting behavior after SYNJ2BP silencing

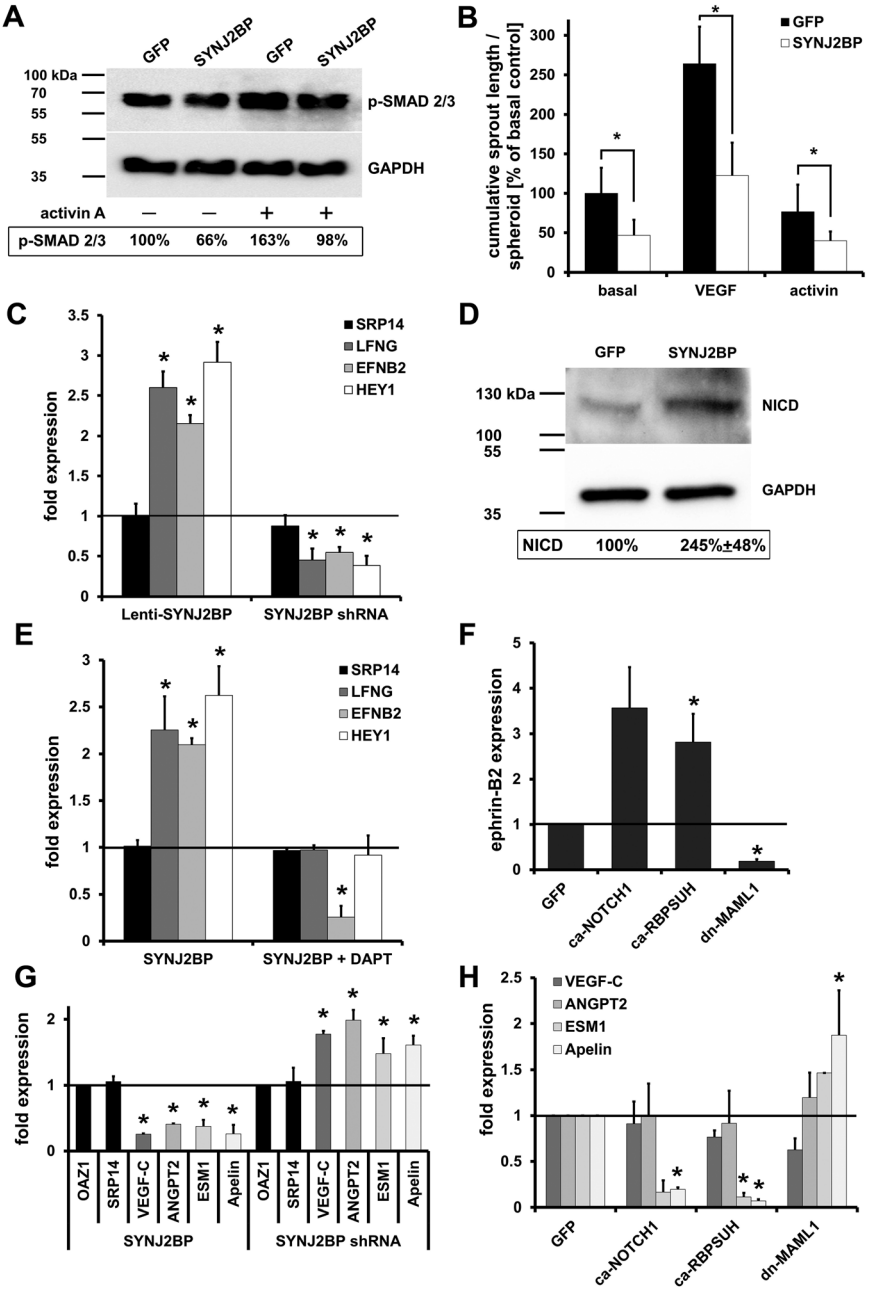

Figure 6. Synaptojanin-2 binding protein (SYNJ2BP) regulates Notch signaling. A, Western blot showing how SMAD 2/3 phosphorylation is regulated by SYNJ2BP and activin A. Human umbilical vein endothelial cells (HUVECs) expressing green fluorescent protein (GFP) or SYNJ2BP were treated with 10 ng/mL activin-A for 24 h. Band quantification showed that activin-A increased SMAD 2/3 phosphorylation. SYNJ2BP had a negative effect, confirming that SYNJ2BP opposes activin signaling. **B**, In a spheroid-based sprouting assay, SYNJ2BP and activin A (25 ng/mL) had additive effects in inhibiting sprouting angiogenesis. Ten spheroids per condition. **C**, Quantitative polymerase chain reaction (qPCR) analysis of HUVECs 48 h after shRNA-mediated SYNJ2BP silencing or lentiviral SYNJ2BP overexpression revealed that ephrin-B2 and the Notch target genes HEY1 and lunatic fringe (LFNG) are regulated by SYNJ2BP. mRNA expression values were normalized to OAZ1 and compared with HUVECs expressing GFP or nonsilencing shRNA. SRP14 served as an additional internal control. n=3. **D**, Western blotting revealed increased levels of cleaved NOTCH1 intracellular domain (NICD), indicating active Notch signaling. Cleaved NOTCH1 was augmented by 145% compared with control (n=3). **E**, Blocking of Notch signaling abolished SYNJ2BP effects on Notch target genes. qPCR analysis showing that the upregulation of ephrin-B2, HEY1, and LFNG on SYNJ2BP overexpression could be prevented by inhibiting Notch signaling with the γ-secretase inhibitor N-[(3,5-difluorophenyl)acetyl]-L-alanyl-2-phenyl]glycine-1,1-dimethylethylester. mRNA expression values were normalized to OAZ1 expression. **F**, Ephrin-B2 is a Notch target gene. The mRNA expression levels of ephrin-B2 in HUVECs, which expressed constitutively active NOTCH1 (NICD), constitutively active RBPSUH (RBPJκ-VP16), or dominant-negative Mastermind-like 1 (dn-MAML1), indicated that ephrin-B2 expression was regulated by Notch signaling. Expression values were normalized to HPRT1. n=3. **G**, qPCR analysis showing that the expression of VEGF-C and typical tip cell markers ANGPT2, ESM1, and Apelin were reduced by forced SYNJ2BP expression and increased by SYNJ2BP silencing in HUVECs. Expression values were normalized to OAZ1. n=3. **H**, qPCR analysis revealed that the expression of VEGF-C and ANGPT2 was not significantly altered by manipulation of Notch signaling in HUVECs. Expression of ESM1 and Apelin depended on Notch signaling. Expression values were normalized to OAZ1. n=2. Results are expressed as means±SD (**B**–**E**, **G**, **H**), or means±SE (**F**). *P<0.05.

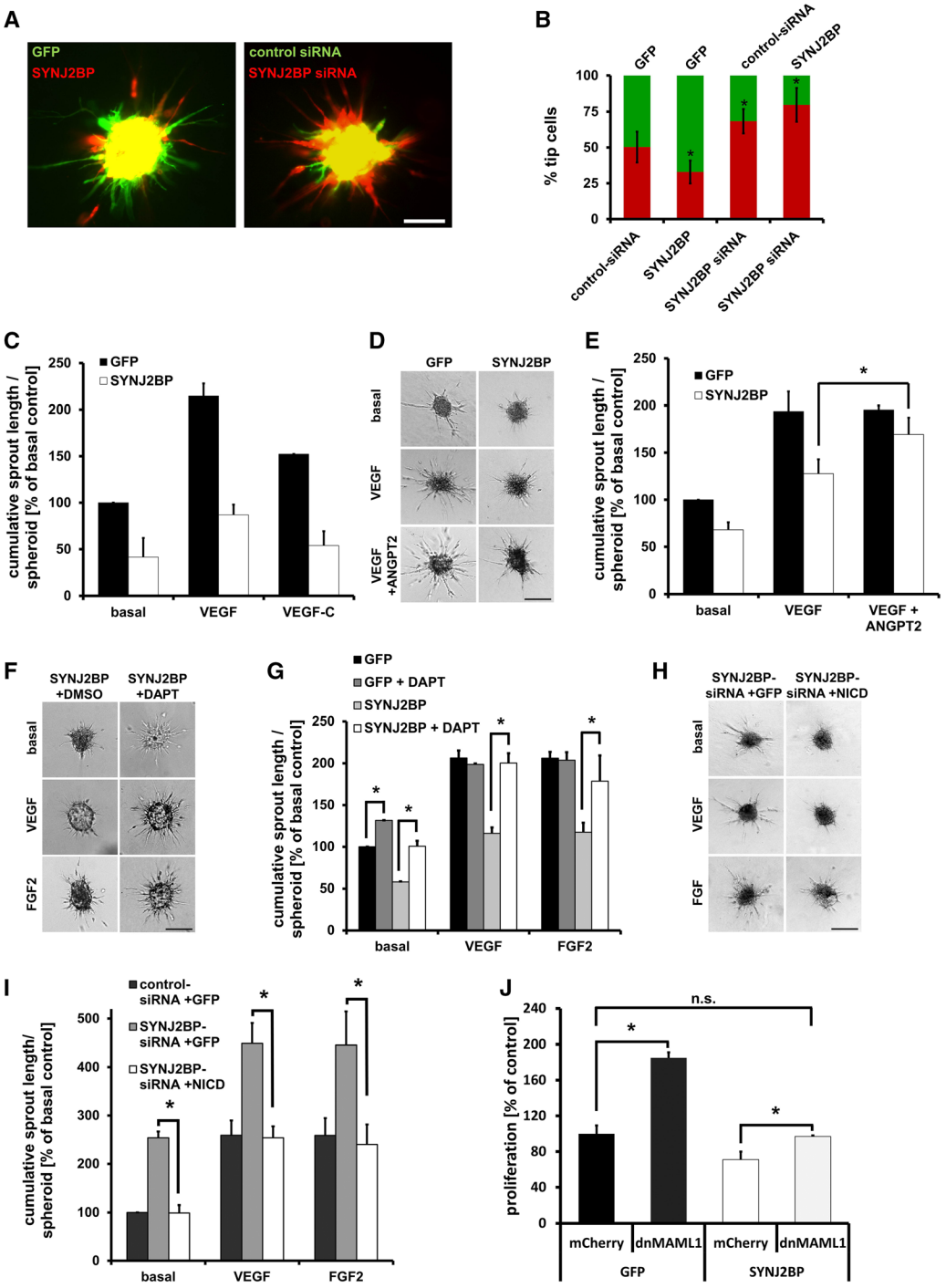

Figure 7. Antiangiogenic effects of Synaptojanin-2 binding protein (SYNJ2BP) are mediated by Notch signaling. A, Example images showing how manipulation of SYNJ2BP expression influences human umbilical vein endothelial cell (HUVEC) sprouting behavior. Control HUVECs (green fluorescent protein or control siRNA; green) and SYNJ2BP-expressing or silenced HUVECs (CellTracker; red) were mixed in equal amounts in a spheroid-based sprouting assay. Fluorescence imaging was performed with a phase-contrast microscope (Olympus IX71). Scale bar, 50 μm. **B**, Quantification of n≥34 spheroids per condition revealed that SYNJ2BP significantly inhibited cells from being localized at the tip cell position. Results are expressed as mean±SD. **C**, SYNJ2BP expression in HUVEC spheroids inhibited vascular endothelial growth factor (VEGF) and FGF2-induced sprouting. This could not be increased back to normal levels by treatment with recombinant VEGF-C (30 ng/mL) for 24 h. Ten spheroids per condition. **D**, Treatment of HUVECs with recombinant human ANGPT2 (200 ng/mL) markedly reinforced the sprouting capacity of SYNJ2BP-expressing cells in the spheroid-based sprouting assay. Scale bar, 100 μm. **E**, Quantification of 3 individual assays with 10 spheroids each. **F**, The antiangiogenic effects of SYNJ2BP were ameliorated by Notch inhibition with the γ-secretase inhibitor N-[(3,5-difluorophenyl)acetyl]-L-alanyl-2-phenyl]glycine-1,1-dimethylethylester (25 μmol/mL in DMSO). Scale bar, 100 μm. **G**, Quantification of 3 individual assays, 10 spheroids each. **H**, Forced Notch activity by adenoviral NICD expression normalized sprouting angiogenesis after lentiviral SYNJ2BP silencing. Scale bar, 100 μm. **I**, Quantification of 3 individual experiments. Images were visualized with the phase-contrast microscope (Olympus IX50). **J**, Inhibition of Notch signaling by expression of dominant-negative Mastermind-like 1 (dn-MAML1) diminished the antiproliferative effects of increased SYNJ2BP expression in HUVECs. n=3 independent experiments, 5 wells per condition. Results are expressed as means+SD. *P<0.05.

(Figure 7H and 7I). Moreover, the effects of SYNJ2BP on endothelial cell proliferation could also be rescued by dominant-negative Mastermind-like 1 protein (Figure 7J). This indicates that ANGPT2 and Notch signaling are 2 crucial, independent signaling cascades downstream of SYNJ2BP.

SYNJ2BP Stabilizes the Notch Ligands DLL1 and DLL4

The question arose how the physical binding of SYNJ2BP to DLL1 and DLL4 could enhance Notch signaling in endothelial cells. SYNJ2BP enhances the endocytosis of activin type II receptors.[19] Because Notch ligand endocytosis is essential for Notch activation,[7] we investigated whether SYNJ2BP expression influences the endocytosis rate of DLL1 (analysis of DLL4 failed because of a lack of suitable antibodies) during normal culture conditions. An immortalized HUVEC line was stably infected with lentivirus expressing DLL1. The internalization rate of membrane surface proteins was determined with a biotinylation/debiotinylation assay[39] after SYNJ2BP or GFP expression. The internalization rate of DLL1 proteins was not significantly altered (Online Figure VA). However, we detected that the amount of membrane-bound DLL1 protein was higher in SYNJ2BP-expressing cells (Online Figure VB).

This intrigued us, so we tried to determine DLL1 and DLL4 protein expression on SYNJ2BP expression. Immunostaining of HUVECs revealed that SYNJ2BP expression strongly enhanced the cellular amount of DLL4 protein. DLL4 was localized in intracellular vesicles as well as at the cell membrane (Figure 8A), as expected. Western blotting confirmed increased DLL1 and DLL4 protein expression (Figure 8B; Online Figure VIA). However, this was not because of increased mRNA transcription (Figure 8C). The DLL4 gene is transcribed in oscillatory-like waves on VEGF treatment,[15,16] and this was not altered on SYNJ2BP expression (Figure 8D). These results indicated that SYNJ2BP may promote the stability of DLL1 and DLL4 proteins. The inhibition of protein synthesis by cycloheximide revealed that forced SYNJ2BP expression increased the half-life of DLL4 protein from ≈80 to 180 minutes in HUAEC monolayers (Figure 8E and 8F). SYNJ2BP also increased the half-life of DLL1 protein from 130 to 200 minutes in HUAECs (Figure 8G; Online Figure VIB). Similarly, SYNJ2BP increased the DLL1 half-life from 130 to 190 minutes in HUVECs (Online Figure VIC). This results in an accumulation of Notch ligands, which should be capable of stimulating Notch receptors in trans.

To analyze this, HUVECs were first cocultured with C2C12 myoblasts. It is well-known that the induction of Notch signaling in C2C12 cells inhibits the differentiation of these progenitor cells into muscle cells.[40,41] When HUVECs were cocultured with C2C12 cells, they could not prevent serum-induced differentiation into myocytes. However, SYNJ2BP-expressing HUVECs—exhibiting high DLL4 and DLL1 levels—sufficiently inhibited differentiation of neighboring C2C12 cells (Online Figure VC). Second, we mixed HUVECs silenced for either SYNJ2BP or DLL4 with primary mouse lung endothelial cells and measured Notch target gene expression in the murine cells using species-specific primer pairs. Similar to silencing of DLL4, the reduced amounts of SYNJ2BP in the human cells also led to decreased Notch activity in the adjacent murine cells (Figure 8H). Taken together, these data indicate that SYNJ2BP promotes Delta protein stabilization in endothelial cells, and this induces Notch signaling in endothelial and nonendothelial cells.

SYNJ2BP most likely interferes with the degradation of DLL1 and DLL4. The mode of Notch ligand proteolysis is not fully resolved yet, and degradation through the proteasome or the lysosome is discussed.[42–44] We found no alterations in DLL4 ubiquitinylation on SYNJ2BP expression (Online Figure VD) and, consistently, inhibition of the proteasome did not change the half-life of DLL4 (Figure 8I). However, blockade of lysosome activity prolonged the half-life of DLL4 to approximately the same extent as did SYNJ2BP expression under control conditions. Importantly, SYNJ2BP expression had no additive effect to the lysosome inhibitor (Figure 8J). This could also be observed for DLL1 (Online Figure VID). Therefore, we conclude that SYNJ2BP expression interferes with lysosomal degradation of DLL1 and DLL4; this prolongs its half-life, leading to protein accumulation, in part also at the cell membrane, and increased Notch activity in trans. Notch activity subsequently inhibits angiogenic sprouting and promotes the stalk cell phenotype.

In summary, we suggest that (Online Figure VII) VEGF signaling induces acquisition of the tip cell phenotype, followed by strong transcription of DLL4. The DLL4 protein activates Notch1 in adjacent cells, which adopt the stalk cell phenotype.[8–11] The poor sensitivity of stalk cells toward VEGF eliminates the strongest inducer of DLL4 expression, causing a decline of DLL4 protein expression. However, SYNJ2BP expression in stalk cells stabilizes the DLL1 and DLL4 protein expression, supporting Delta-Notch signaling to occur also within the stalk cell plexus. Such continuous Notch signaling is necessary to prevent the conversion into the tip cell phenotype,[9] to allow further vessel remodeling,[18] and even to prevent angiogenesis in mature vessels.[12,13]

Discussion

Angiogenesis is coordinated by the fine-tuned interplay of pro- and antiangiogenic pathways. VEGF/VEGF receptor, Delta/Notch, Angiopoietin/Tie, Semaphorins/Neuropilins/Plexins, Slit/Robo, and Ephrin/Eph are among the key signaling pathways that guide angiogenic sprouting, but additional factors are needed to fine-tune this complex process.[6] The Notch cascade acts as a central coordinator of vessel outgrowth, critically controlling the selection of sprouting tip cells versus remodeling stalk cells by decreasing VEGF sensitivity of stalk cells. This is of particular interest for antiangiogenic therapy, because Notch inhibition by blocking antibodies or γ-secretase inhibitors leads to excessive angiogenic sprouting and branching with a poorly functional vasculature.[10,11,45,46]

The complexity of Notch signaling is mechanistically still poorly understood. Although Delta-Notch interactions in trans activate the Notch receptors, binding in cis can be antagonistic.[47] Likewise, it has recently been shown that the glycosyltransferase fringe can modify Notch receptors to enhance DLL4-mediated signaling in endothelial cells. Conversely, the Notch ligand JAG1 may antagonize this DLL4-Notch signaling during sprouting angiogenesis.[33] Additionally, several other modifications of Notch signaling can be seen. Notch ligands need to undergo endocytosis to become fully competent to activate Notch receptors.

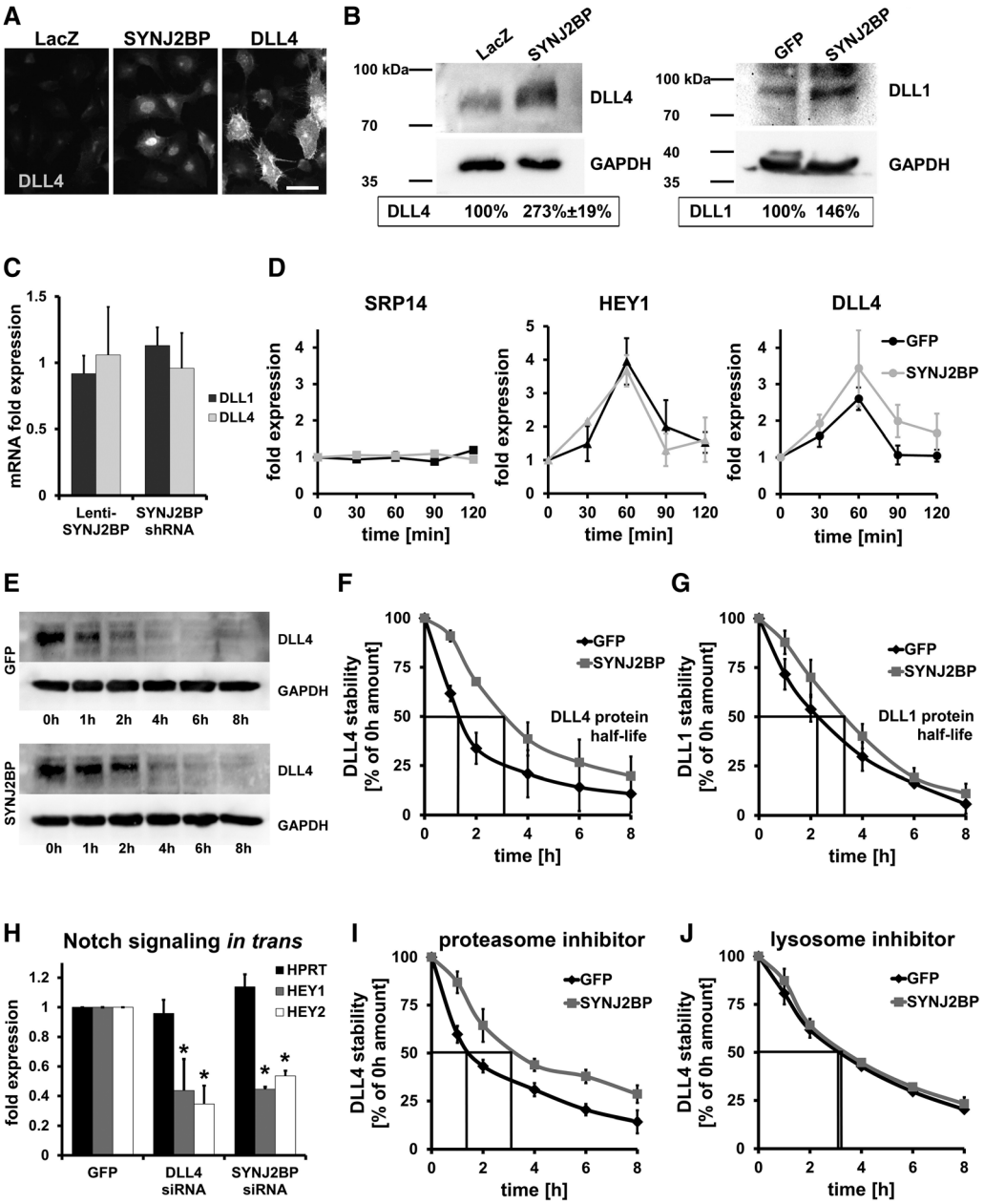

Figure 8. SYNJ2BP promotes endothelial DLL4 protein stability. A, Human umbilical vein endothelial cells (HUVECs) were adenovirally infected with lacZ, SYNJ2BP, or DLL4 and stained for DLL4 protein expression after 48 h. Representative immunofluorescence images are shown. Compared with lacZ as control, SYNJ2BP increased the amount of DLL4 protein (Alexa488). DLL4 gain-of-function was taken as a positive control. DLL4 shows the typical staining pattern predominantly in endosomes and at the membrane. Scale bar, 50 μm. **B**, Western blotting after SYNJ2BP gain-of-function revealed increased DLL4 protein levels compared with lacZ control (273±19%; n=3) and increased DLL1 proteins levels compared with green fluorescent protein (GFP) control. GAPDH was used as loading control. **C**, DLL1 and DLL4 mRNA amounts were not significantly altered by SYNJ2BP expression. Results are expressed as means±SE. n=3. **D**, Quantitative polymerase chain reaction (qPCR) analysis demonstrated that vascular endothelial growth factor (VEGF)-induced DLL4 expression was not significantly altered by SYNJ2BP. HUVECs expressing GFP or SYNJ2BP were stimulated with VEGF-A (25 ng/mL) at 0 min; mRNA was harvested at the indicated time points. VEGF induced expression of HEY1 and DLL4, but not of the control SRP14. Expression values were normalized to OAZ1; n=3. Results are expressed as means±SD. **E**, Forty-eight hours after viral infection, human umbilical artery endothelial cells were cultured in the presence of 0.1 mmol/L cycloheximide to block protein synthesis (time point 0 h). Western blotting of protein lysates at different time points showed increased stability of DLL4 protein. **F**, Quantification of Western blot bands indicated decreased degradation rates and extended half-life for DLL4 in the presence of SYNJ2BP (180 min compared with 80 min in the control). The effect on DLL4 stability was statistically significant (tested with a 2-way ANOVA; $P<0.05$); n=3. Results are expressed as means±SD. **G**, Quantification of Western blot bands of a cycloheximide assay depicted slightly increased DLL1 protein stability with forced expression of SYNJ2BP (200 min compared with 130 min); n=3. Results are expressed as means±SD. **H**, HUVECs were cocultured with murine endothelial cells. qPCR analysis with species-specific primers showed that Notch target gene expression was reduced when HUVECs were silenced for DLL4 or SYNJ2BP. Expression levels were normalized to GAPDH; n=3. Results are expressed as means±SD. *$P<0.05$. **I**, Quantification of Western blot bands of DLL4 half-life conducted in presence of the proteasome inhibitor lactacystin (1 μmol/L). SYNJ2BP overexpression increases DLL4 half-life from 90 to 190 min; n=3. Results are expressed as means±SD. **J**, In presence of the lysosome inhibitor chloroquine (300 μmol/L), DLL4 half-life was 200 min and 190 min with and without SYNJ2BP overexpression, respectively; n=3. Results are expressed as means±SD.

This study was aimed at identifying novel modifying factors of Notch signaling through a yeast 2-hybrid screen. This approach and subsequent validation experiments identified the membrane-associated guanylate kinase homologue proteins MAGI2 and MAGI3, the multiple PDZ domain protein MUPP1, as well as the PDZ domain protein SYNJ2BP (ARIP2) as novel interaction partners of DLL1 and DLL4. MAGI1 has previously been reported to bind the PDZ peptide of DLL1.[26] All of the isolated interaction partners were PDZ domain proteins. Thus, it can be assumed that there are multiple ways PDZ proteins bind or compete for binding to Notch ligands. It can be seen that Notch ligands behave differently depending on the actual intracellular binding partner.

The biochemical and angiogenesis-regulating functions of SYNJ2BP in endothelial cells were subsequently studied in more detail. The physical interaction with Delta ligands appeared to stimulate Notch signaling. SYNJ2BP enhanced the expression of DLL4 protein as shown by Western blotting and immunostaining. This was independent of gene transcription. SYNJ2BP bound to DLL4, and this interaction stabilized the Notch ligand and extended its half-life from 80 to 180 minutes, probably by inhibition of lysosomal degradation. Similarly, the cell surface DLL1 protein levels were increased as DLL1 was stabilized by SYNJ2BP, although to a lesser extent compared with DLL4. This allowed SYNJ2BP-expressing endothelial cells to stimulate neighboring cells carrying Notch receptors. In this regard, Notch signaling was enhanced not only in endothelial cells but also in C2C12 myoblasts that were cocultured with SYNJ2BP-expressing HUVECs. Thus, the recruitment of SYNJ2BP appears as a novel mechanism to stabilize Delta ligands and to allow increased activation of Notch receptor-carrying cells.

Functionally, SYNJ2BP phenocopied Delta-Notch signaling in endothelial cells. Overexpression of this PDZ protein inhibited endothelial proliferation, migration, and sprouting angiogenesis. The data suggest that SYNJ2BP expression promotes the stalk cell phenotype[6] with high Notch activity and LFNG expression. Fringe glycosyltransferases can modify Notch receptors to sensitize them to Delta ligands in endothelial cells.[33] Consistently, expression of the tip cell molecule ANGPT2[37] was strongly reduced and the tip cell promoting VEGF factors were less active when added to SYNJ2BP-expressing cells.

The present study furthermore demonstrated that SYNJ2BP acts as an antiangiogenic molecule in vivo. To unravel antiangiogenic functions of SYNJ2BP, we implanted SYNJ2BP-silenced human endothelial cells in a growth factor–rich matrix subcutaneously in immunocompromised mice. This xenotransplantation technique allows the formation of a human vasculature in mice, which anastomoses with the mouse vasculature, becomes perfused, and matures by recruitment of host mural cells. The assay has previously been validated as a powerful in vivo system to study effects of vascular growth factors and inhibitors[24] and also to genetically modify the angiogenic program.[4,23] Silencing of SYNJ2BP expression led to a significant increase in blood vessel density, indicating that SYNJ2BP acts as a negative regulator of angiogenesis, preventing uncontrolled angiogenesis in a Notch-dependent manner. In vivo DLL4 blockade leads to increased microvessel density combined with lesser vessel perfusion in grafted tumors.[11] In this study, we showed that SYNJ2BP is capable of modifying Notch signaling in such a way that it phenocopies most of the effects seen after DLL4-Notch manipulation. Because SYNJ2BP can also influence activin signaling, and because SYNJ2BP and DLL4 expression patterns only partially overlap,[19,20] it is obvious that its inhibition cannot completely resemble every single aspect of a DLL4-Notch loss. In summary, the present study identified SYNJ2BP as a novel binding protein of the Notch ligands DLL1 and DLL4, which led to stabilization and accumulation of both Delta-like proteins and activation of Notch signaling. Consistently, SYNJ2BP restrained growth factor–induced angiogenesis in vitro and in vivo.

Acknowledgments

We thank the members of the Fischer laboratory for fruitful discussions. We are grateful to Dr Achim Gossler, Hannover, Germany, for providing DLL1 antibodies.

Sources of Funding

This work was supported by grants from the SFB/Transregio 23 (to A.F. and H.G.A.) and the Chica and Heinz Schaller Foundation (to A.F).

Disclosures

None.

References

1. Carmeliet P, Jain RK. Molecular mechanisms and clinical applications of angiogenesis. *Nature*. 2011;473:298–307.
2. Li WW, Hutnik M, Gehr G. Antiangiogenesis in haematological malignancies. *Br J Haematol*. 2008;143:622–631.
3. Rosenfeld PJ, Brown DM, Heier JS, Boyer DS, Kaiser PK, Chung CY, Kim RY; MARINA Study Group. Ranibizumab for neovascular age-related macular degeneration. *N Engl J Med*. 2006;355:1419–1431.
4. Wüstehube J, Bartol A, Liebler SS, Brütsch R, Zhu Y, Felbor U, Sure U, Augustin HG, Fischer A. Cerebral cavernous malformation protein CCM1 inhibits sprouting angiogenesis by activating DELTA-NOTCH signaling. *Proc Natl Acad Sci U S A*. 2010;107:12640–12645.
5. Augustin HG, Koh GY, Thurston G, Alitalo K. Control of vascular morphogenesis and homeostasis through the angiopoietin-Tie system. *Nat Rev Mol Cell Biol*. 2009;10:165–177.
6. Herbert SP, Stainier DY. Molecular control of endothelial cell behaviour during blood vessel morphogenesis. *Nat Rev Mol Cell Biol*. 2011;12:551–564.
7. Kopan R, Ilagan MX. The canonical Notch signaling pathway: unfolding the activation mechanism. *Cell*. 2009;137:216–233.
8. Phng LK, Gerhardt H. Angiogenesis: a team effort coordinated by notch. *Dev Cell*. 2009;16:196–208.
9. Hellström M, Phng LK, Hofmann JJ, et al. Dll4 signalling through Notch1 regulates formation of tip cells during angiogenesis. *Nature*. 2007;445:776–780.
10. Noguera-Troise I, Daly C, Papadopoulos NJ, Coetzee S, Boland P, Gale NW, Lin HC, Yancopoulos GD, Thurston G. Blockade of Dll4 inhibits tumour growth by promoting non-productive angiogenesis. *Nature*. 2006;444:1032–1037.
11. Ridgway J, Zhang G, Wu Y, et al. Inhibition of Dll4 signalling inhibits tumour growth by deregulating angiogenesis. *Nature*. 2006;444:1083–1087.
12. Liu Z, Turkoz A, Jackson EN, Corbo JC, Engelbach JA, Garbow JR, Piwnica-Worms DR, Kopan R. Notch1 loss of heterozygosity causes vascular tumors and lethal hemorrhage in mice. *J Clin Invest*. 2011;121:800–808.
13. Yan M, Callahan CA, Beyer JC, Allamneni KP, Zhang G, Ridgway JB, Niessen K, Plowman GD. Chronic DLL4 blockade induces vascular neoplasms. *Nature*. 2010;463:E6–E7.
14. Jakobsson L, Franco CA, Bentley K, Collins RT, Ponsioen B, Aspalter IM, Rosewell I, Busse M, Thurston G, Medvinsky A, Schulte-Merker S, Gerhardt H. Endothelial cells dynamically compete for the tip cell position during angiogenic sprouting. *Nat Cell Biol*. 2010;12:943–953.
15. Beets K, Huylebroeck D, Moya IM, Umans L, Zwijsen A. Robustness in angiogenesis: notch and BMP shaping waves. *Trends Genet*. 2013;29:140–149.
16. Larrivée B, Prahst C, Gordon E, del Toro R, Mathivet T, Duarte A, Simons M, Eichmann A. ALK1 signaling inhibits angiogenesis by cooperating with the Notch pathway. *Dev Cell*. 2012;22:489–500.

17. Hofmann JJ, Luisa Iruela-Arispe M. Notch expression patterns in the retina: an eye on receptor-ligand distribution during angiogenesis. *Gene Expr Patterns*. 2007;7:461–470.
18. Lobov IB, Cheung E, Wudali R, Cao J, Halasz G, Wei Y, Economides A, Lin HC, Papadopoulos N, Yancopoulos GD, Wiegand SJ. The Dll4/Notch pathway controls postangiogenic blood vessel remodeling and regression by modulating vasoconstriction and blood flow. *Blood*. 2011;117:6728–6737.
19. Matsuzaki T, Hanai S, Kishi H, Liu Z, Bao Y, Kikuchi A, Tsuchida K, Sugino H. Regulation of endocytosis of activin type II receptors by a novel PDZ protein through Ral/Ral-binding protein 1-dependent pathway. *J Biol Chem*. 2002;277:19008–19018.
20. Nemoto Y, De Camilli P. Recruitment of an alternatively spliced form of synaptojanin 2 to mitochondria by the interaction with the PDZ domain of a mitochondrial outer membrane protein. *EMBO J*. 1999;18:2991–3006.
21. Liu HY, Chen FF, Ge JY, Wang YN, Zhang CH, Cui XL, Yu F, Tai GX, Liu ZH. Expression and localization of activin receptor-interacting protein 2 in mouse tissues. *Gen Comp Endocrinol*. 2009;161:276–282.
22. Li ZD, Wu Y, Bao YL, Yu CL, Guan LL, Wang YZ, Meng XY, Li YX. Identification and characterization of human ARIP2 and its relation to breast cancer. *Cytokine*. 2009;46:251–259.
23. Brütsch R, Liebler SS, Wüstehube J, Bartol A, Herberich SE, Adam MG, Telzerow A, Augustin HG, Fischer A. Integrin cytoplasmic domain-associated protein-1 attenuates sprouting angiogenesis. *Circ Res*. 2010;107:592–601.
24. Alajati A, Laib AM, Weber H, Boos AM, Bartol A, Ikenberg K, Korff T, Zentgraf H, Obodozie C, Graeser R, Christian S, Finkenzeller G, Stark GB, Héroult M, Augustin HG. Spheroid-based engineering of a human vasculature in mice. *Nat Methods*. 2008;5:439–445.
25. Laib AM, Bartol A, Alajati A, Korff T, Weber H, Augustin HG. Spheroid-based human endothelial cell microvessel formation in vivo. *Nat Protoc*. 2009;4:1202–1215.
26. Mizuhara E, Nakatani T, Minaki Y, Sakamoto Y, Ono Y, Takai Y. MAGI1 recruits Dll1 to cadherin-based adherens junctions and stabilizes it on the cell surface. *J Biol Chem*. 2005;280:26499–26507.
27. Pfister S, Przemeck GK, Gerber JK, Beckers J, Adamski J, Hrabé de Angelis M. Interaction of the MAGUK family member Acvrinp1 and the cytoplasmic domain of the Notch ligand Delta1. *J Mol Biol*. 2003;333:229–235.
28. Chen JR, Chang BH, Allen JE, Stiffler MA, MacBeath G. Predicting PDZ domain-peptide interactions from primary sequences. *Nat Biotechnol*. 2008;26:1041–1045.
29. Barrios-Rodiles M, Brown KR, Ozdamar B, et al. High-throughput mapping of a dynamic signaling network in mammalian cells. *Science*. 2005;307:1621–1625.
30. Hammes HP, Brownlee M, Jonczyk A, Sutter A, Preissner KT. Subcutaneous injection of a cyclic peptide antagonist of vitronectin receptor-type integrins inhibits retinal neovascularization. *Nat Med*. 1996;2:529–533.
31. Qi Y, Ge JY, Wang YN, Liu HY, Li YM, Liu ZH, Cui XL. Co-expression of activin receptor-interacting protein 1 and 2 in mouse nerve cells. *Neurosci Lett*. 2013;542:53–58.
32. Krneta J, Kroll J, Alves F, Prahst C, Sananbenesi F, Dullin C, Kimmina S, Phillips DJ, Augustin HG. Dissociation of angiogenesis and tumorigenesis in follistatin- and activin-expressing tumors. *Cancer Res*. 2006;66:5686–5695.
33. Benedito R, Roca C, Sörensen I, Adams S, Gossler A, Fruttiger M, Adams RH. The notch ligands Dll4 and Jagged1 have opposing effects on angiogenesis. *Cell*. 2009;137:1124–1135.
34. Sawamiphak S, Seidel S, Essmann CL, Wilkinson GA, Pitulescu ME, Acker T, Acker-Palmer A. Ephrin-B2 regulates VEGFR2 function in developmental and tumour angiogenesis. *Nature*. 2010;465:487–491.
35. Wang Y, Nakayama M, Pitulescu ME, Schmidt TS, Bochenek ML, Sakakibara A, Adams S, Davy A, Deutsch U, Lüthi U, Barberis A, Benjamin LE, Mäkinen T, Nobes CD, Adams RH. Ephrin-B2 controls VEGF-induced angiogenesis and lymphangiogenesis. *Nature*. 2010;465:483–486.
36. Iso T, Maeno T, Oike Y, Yamazaki M, Doi H, Arai M, Kurabayashi M. Dll4-selective Notch signaling induces ephrinB2 gene expression in endothelial cells. *Biochem Biophys Res Commun*. 2006;341:708–714.
37. del Toro R, Prahst C, Mathivet T, Siegfried G, Kaminker JS, Larrivee B, Breant C, Duarte A, Takakura N, Fukamizu A, Penninger J, Eichmann A. Identification and functional analysis of endothelial tip cell-enriched genes. *Blood*. 2010;116:4025–4033.
38. Felcht M, Koenen W, Weiss C, Weina K, Geraud C, Faulhaber J. Delayed closure of complex defects with serial tightening of loop sutures - clinical outcome in 64 consecutive patients. *J Eur Acad Dermatol Venereol*. 2013 Mar 5 [Epub ahead of print].
39. Roberts M, Barry S, Woods A, van der Sluijs P, Norman J. PDGF-regulated rab4-dependent recycling of alphavbeta3 integrin from early endosomes is necessary for cell adhesion and spreading. *Curr Biol*. 2001;11:1392–1402.
40. Dahlqvist C, Blokzijl A, Chapman G, Falk A, Dannaeus K, Ibáñez CF, Lendahl U. Functional Notch signaling is required for BMP4-induced inhibition of myogenic differentiation. *Development*. 2003;130:6089–6099.
41. Nofziger D, Miyamoto A, Lyons KM, Weinmaster G. Notch signaling imposes two distinct blocks in the differentiation of C2C12 myoblasts. *Development*. 1999;126:1689–1702.
42. Chapman G, Sparrow DB, Kremmer E, Dunwoodie SL. Notch inhibition by the ligand DELTA-LIKE 3 defines the mechanism of abnormal vertebral segmentation in spondylocostal dysostosis. *Hum Mol Genet*. 2011;20:905–916.
43. Dyczynska E, Sun D, Yi H, Sehara-Fujisawa A, Blobel CP, Zolkiewska A. Proteolytic processing of delta-like 1 by ADAM proteases. *J Biol Chem*. 2007;282:436–444.
44. Koutelou E, Sato S, Tomomori-Sato C, Florens L, Swanson SK, Washburn MP, Kokkinaki M, Conaway RC, Conaway JW, Moschonas NK. Neuralized-like 1 (Neurl1) targeted to the plasma membrane by N-myristoylation regulates the Notch ligand Jagged1. *J Biol Chem*. 2008;283:3846–3853.
45. Sainson RC, Aoto J, Nakatsu MN, Holderfield M, Conn E, Koller E, Hughes CC. Cell-autonomous notch signaling regulates endothelial cell branching and proliferation during vascular tubulogenesis. *FASEB J*. 2005;19:1027–1029.
46. Wu Y, Cain-Hom C, Choy L, et al. Therapeutic antibody targeting of individual Notch receptors. *Nature*. 2010;464:1052–1057.
47. Sprinzak D, Lakhanpal A, Lebon L, Santat LA, Fontes ME, Anderson GA, Garcia-Ojalvo J, Elowitz MB. Cis-interactions between Notch and Delta generate mutually exclusive signalling states. *Nature*. 2010;465:86–90.

Novelty and Significance

What Is Known?

- The outgrowth of a new blood vessel is guided by a group of leading tip cells, which are followed by stalk cells.
- Vascular endothelial growth factor (VEGF) induces tip cell formation and expression of the DLL4 protein.
- DLL4 signals to adjacent cells and induces Notch signaling, which promotes the stalk cell phenotype. The related DLL1 protein signals to Notch receptors within the stalk cell plexus.

What New Information Does This Article Contribute?

- Synaptojanin-2 binding protein (SYNJ2BP) was identified as a novel binding protein to DLL1 and DLL4 that prolongs their half-life and enforces Notch signaling.
- SYNJ2BP is predominantly expressed in the stalk cell plexus.
- SYNJ2BP inhibits tip cell formation and vessel sprouting.

Sprouting angiogenesis requires the coordinated response of endothelial cells toward growth factors like VEGF. Delta-Notch signaling has emerged as a major regulator for selection of the tip cells that are responsive to VEGF. In contrast, Notch activity decreases sensitivity of the trailing stalk cells to VEGF. This coordination restricts vessel branching and allows formation of a functional vessel network. This study identified a novel regulator of Notch signaling during angiogenesis. SYNJ2BP expression in endothelial cells promotes strong Notch signaling between neighboring cells. This prevents tip cell formation and further vessel branching. Our results introduce a novel mechanism of sprouting angiogenesis regulation via controlling the Notch ligand half-life.

SUPPLEMENTAL MATERIAL

Synaptojanin-2 binding protein stabilizes the Notch ligands DLL1 and DLL4 and inhibits sprouting angiogenesis

Detailed Methods

Yeast Two-Hybrid assay

The screening was performed as described,[1] using the MATCHMAKER Gal4 system (Clontech). Yeast strain AH109 was transformed with the bait plasmid pGBK-DLL1-ic and pGBK-DLL4-ic, respectively. Both baits showed no signs of toxicity or autoactivation of reporter genes. The AH109 strain was mated with the Y187 strain carrying a mouse embryo E13 cDNA library (Clontech). Colonies surviving on agar plates lacking adenine, histidine, leucine, and tryptophan were isolated. Duplicates were eliminated by colony PCR and HaeIII digest, the prey plasmids were isolated and transformed into Y187. False-positive clones were eliminated according to the manufacturer's protocol and the remaining ones sequenced.

Cell culture

Human umbilical vein endothelial cells (HUVEC) were freshly prepared from umbilical veins and grown in ECGM2 with SupplementMix (PromoCell, Heidelberg, Germany) and 10% heat inactivated FCS (Biochrom) or Endopan (Endopan 3 Kit, Pan-Biotech, Heidelberg, Germany) containing 1% penicillin/streptomycin. For preparation umbilical veins were flushed with PBS and filled with collagenase (1 mg/ml) for 15 min at 37 °C. Cells were harvested, centrifuged and seeded in 10 ml medium in a 75 cm^2 flask. At passage 1 endothelial identity was verified by CD31 (JC70A, DAKO) and αSMA (1A4, DAKO) immunostaining. Cells were seeded on glass cover slips, fixed with 4% paraformaldehyde, stained with primary antibodies (1:25) for 1 h and secondary Alexa 546-coupled antibodies (Molecular Probes) for 30 min. HUVEC of passages 3-6 were used for experiments.

For virus production HEK293 cells (ATCC) were used that were cultured in DMEM (Dulbecco's modified Eagle medium, Gibco) supplemented with 10% heat inactivated FCS.

Murine lung endothelial cells (mLEC) were isolated using a magnetic cell separation method from C57BL/6 mice as previously described[2] and grown in the same medium as HUVEC. mLEC of passage 3 were used for the experiments.

Plasmids, siRNA, and shRNA

A human SYNJ2BP cDNA cassette in pDONR223 (GenBank: BC007704) was used for Gateway cloning into adenoviral (pAd-V5-DEST) and lentiviral (pLenti6.2-V5-DEST) expression vectors (Invitrogen). Full length murine Synj2bp cDNA (GenBank: NM025292.6) was PCR amplified (primers see **suppl. Table I**) from an embryonic cDNA library, digested with EcoRI and BamHI, and ligated into pENTR3c (Invitrogen) which contained an IRES-EGFP cassette from pIRES2-EGFP (Clontech). Full length human DLL1 in pENTR223.1 was from OpenBiosystems

(OHS4559-99847851). Full length human DLL4 was transferred to pENTR3c (Invitrogen). For the LUMIER interaction assay, the cDNA inserts were shuttled into pT-REx-DEST30-ctProteinA and pcDNA3-ntRenLuc-GW by Gateway cloning. DLL1 and DLL4 intracellular domains (ic) with and without a functional carboxyterminal PDZ binding domain (lacking amino acids ATEV) were PCR amplified from a cDNA library, digested with BamHI and ligated into pCS2p-FLAG. The inserts were subcloned into the yeast 2-hybrid vectors pGBKT7 and pGADT7 (Invitrogen). Plasmids were controlled by sequencing.
Short hairpin RNA expression vectors against SYNJ2BP (RHS4531-NM_018373) and a non-silencing control were obtained from OpenBiosystems in the lentiviral pGIPZ vector. Pooled siRNA duplexes against human SYNJ2BP (ON-TARGETplus SMARTpool, Gene ID: 55333) were from Thermo Scientific Dharmacon.

HUVEC transfection, transduction, and immunostaining

HUVEC ($1.2x10^5$ cells) were transfected with 200 nmol/l annealed siRNA duplexes in a 6 well plate with 6 µl Oligofectamine (Invitrogen) according to the manufacturer's protocol. Medium was replaced after 4 h with normal growth medium. Lentiviruses and adenoviruses were generated in HEK293 cells. Generation, amplification, and titering were performed according to the ViraPower Adenoviral or Lentiviral Expression System (Invitrogen) protocols. Semiconfluent HUVEC were transduced with multiplicity of infection (MOI) of 10 for lentivirus and MOI of 50 for adenovirus. HUVEC were seeded on gelatine-coated cover slips for immunostaining. 48 h after adenoviral transfection cells were fixed with 4% paraformaldehyde and permeabilized with 0.3% TritonX-100. DLL4 protein was localized using an anti-DLL4 antibody (#2589, Cell Signaling,1:100) and Alexa Fluor 488- or 546-coupled secondary antibodies (Molecular Probes). SYNJ2BP was visualized with a SYNJ2BP antibody (ab69431, Abcam). Nuclei were stained with DAPI. Images were taken with a Leica laser confocal microscope (LSM SP5 DS).

Murine retina and embryo staining

C57BL/6 mice were sacrificed at postnatal day 5 and the eyes were fixed for 10 min in -20°C methanol. Retinae were isolated and permeabilized in 1% BSA and 0.3% Triton X-100 for 2 h at room temperature and washed in PBLEC buffer (1% Triton X-100, 0.1 mM $MgCl_2$, 0.1 mM $CaCl_2$, 0.1 mM $MnCl_2$ in PBS pH 6.8), then incubated overnight in PBLEC plus isolectin-B4 (Sigma-Aldrich), and/or antibodies against SYNJ2BP (ab69431, Abcam), CD31 (Mec13.3, #553370, BD Pharmingen), or Dll4 (#2589, Cell Signaling). After washing, retinae were incubated with secondary antibodies (Invitrogen), washed, and mounted on slides with Fluorescent Mounting Medium (Dako) for visualization using an LSM 700 confocal microscope.
Murine embryos were isolated from C57BL/6 mice at E11.5, fixed with PFA, and embedded in paraffin. Deparaffinized embryo sections (5 µm) were blocked in Tris buffer containing 0.25% Casein and 0.1% BSA and permeabilized with 0.1% Triton-X-100. Primary antibodies against SYNJ2BP (ab69431, Abcam) and CD31 (Mec13.3, #553370, BD Pharmingen) were diluted in blocking buffer and incubated with the samples for 18 h at 4°C. After washing, sections were incubated with secondary antibodies for 2 h, then for additional 10 min with DAPI and mounted with Fluorescent Mounting Medium (Dako). Images were taken using an LSM 700 confocal microscope.

Retinopathy of prematurity model

The retinopathy of prematurity model was used as published by us.[3] Briefly, newborn C57BL/6J mice were exposed to 75% oxygen from postnatal day 7 to postnatal day 12 with their nursing mothers. On the 12th day the mice were returned to room air. Littermate mice without exposure to oxygen served as negative controls. On postnatal day 17 the mice were sacrificed. From each mouse, the retina from one eye was isolated and lysed with trizol employing a syringe and needle. RNA was isolated and dissolved in H_2O. Reverse transcription and qPCR were performed as described below. The other retina was fixed and stained with lectin to confirm the hypoxia-induced increased angiogenesis.

Spheroid-based sprouting assay

This assay was performed as described.[4] In short, HUVEC were trypsinized and suspended in growth medium with 20% methocel (Sigma-Aldrich) 48 h after siRNA transfection or viral transduction. Cells (25 µl) were incubated as hanging drops for 24 h. A spheroid with 400 cells formed in each hanging drop during that time. Spheroids were harvested, suspended in 2 ml methocel with 20% FCS and 2 ml rat collagen and embedded in a 24 well plate. Following polymerization for 30 min, 0.1 ml basal culture medium was added to assess basal sprouting, while VEGF or FGF2 (final concentration 25 ng/ml) was added for stimulation. Cells were fixed after 24 h with 10% formaldehyde. The lengths of all sprouts of at least 10 spheroids per condition were counted using an inverted microscope (Olympus IX50 with cell^P software). The small chemical inhibitor of NOTCH signaling DAPT (Calbiochem) was used at 25 µM. Recombinant human VEGF-C was used at 30 ng/ml, recombinant human ANGPT2 at 200 ng/ml, activin A at 25 ng/ml.

For the two-colored spheroid-based sprouting assay, HUVEC were either transfected with GFP adenovirus as described above or stained with CellTracker™ Red CMTPX (Life Technologies) according to the manufacturer's protocol.

Generation of SYNJ2BP-deficient mice

Mouse embryonic stem cells (RRB066) were purchased from BayGenomics, which carried a mutation in the first intron of the gene *synj2bp* introduced with the gene trapping method. The cells were cultured and tested for pathogens, injected into blastocysts from C57BL/6J mice, and implanted into the uterus of a foster mother, which gave birth to chimeric mice, one of which showed germline transmission. Subsequently the mouse line was backcrossed to a CB57BL/6J background. The homozygous transgenic mice were born at a normal Mendelian ratio and displayed no obvious phenotype. mRNA was harvested from the tissue of the offspring and transcribed to test for a null allele. However insertion of the genetrap did not result in a null allele, since we could still detect gene transcription of exons 2-4. This resulted in a slightly shortened protein, still comprising a full PDZ domain.

***In vivo* spheroid-based angiogenesis assay**

This assay allows the formation of a functional human vasculature in SCID mice and was performed as described.[5, 6] In short, HUVEC (pooled; Lonzal) were infected with lentivirus and

selected with 0.37 µg/ml puromycin. A methocel solution was prepared containing 1.2% carboxymethylcellulose (Sigma-Aldrich) in ECBM. HUVEC were suspended in 20% methocel in growth medium and 25 µl drops, each containing 150 cells, were pipetted on non-adherent plastic petri-dishes to form spheroids in hanging drops. The spheroids were embedded with a 1:1:1 mix of methocel/fibrinogen (2 mg/ml, Calbiochem)/ECGM containing 1 µg/ml VEGF-A 165 and FGF2. This mix was diluted immediately prior to injection 1:1 with growth factor reduced Matrigel (BD Biosciences) and 1 U/µl thrombin (Calbiochem) to initiate polymerization. Spheroids (1,500 per mouse) were injected s.c. into the flank of 6-8 week old CB17 SCID mice (Charles River). Plugs were removed after 28 days and fixed in 4% formaldehyde before embedding in paraffin. Of the animals, 50% were injected i.v. with FITC-Dextran (40 kDa, Sigma-Aldrich) 20 min prior to removal of the plugs to determine perfusion of the neovasculature. Paraffin sections (5 µm) were stained with anti human CD34 (QBEND10, Menarini) and anti alpha smooth muscle actin-Cy3 (Sigma-Aldrich). All animal procedures were carried out in accordance with the local committee for animal experiments (RP Karlsruhe – 35-9185.81/G-67/06; G-27/09).

Aortic ring assay

Aortic ring assay was performed as previously described.[7] Briefly, aortae were isolated from C57BL/6 mice (8 weeks) and cut into ~25 rings each. The rings were transduced with GFP or murine SYNJ2BP adenovirus, embedded in a matrigel matrix (BD), and stimulated with 30 ng/ml VEGF (Preprotech). Images were taken after 24 h with a Nikon SMZ800 microscope.

Endothelial migration, proliferation, and adhesion

Cell migration was assessed with a wound healing assay in the presence of 5 µg/ml mitomycin C to block proliferation. µ-Dish 35 mm high Culture-Inserts ibiTreat (ibidi) were placed in a 24 well plate coated with 0.2% gelatin. Following siRNA transfection or viral transduction (after 24 h), HUVEC were trypsinized and 200,000 cells/ml were suspended in growth medium. Of this suspension, 100 µl were placed in each insert half. After 24 h, HUVEC were starved overnight in ECGM2 with 2.5% FCS lacking the SupplementMix. The inserts were removed and the gap width was measured at the indicated time points. The migration rate was calculated as the velocity of the moving cell front in µm/h.

HUVEC proliferation was determined by BrdU incorporation (Cell Proliferation ELISA, Roche). HUVEC (750 per well) were seeded in a 96 well plate in growth medium. After 24 h, 5-bromodeoxyuridine (BrdU) was added for 2 h and newly synthesized DNA was detected with an enzyme-linked BrdU antibody.

Cell adhesion was measured 48 h after siRNA transfection or viral transduction. HUVEC (20,000 per well) were seeded in 50 µl normal growth medium in a 96 well plate which had been coated with fibronectin (20 µg/ml, Sigma-Aldrich), collagen (3 mg/ml), 0.2% gelatin, or water as control. The plates were incubated for 30 min and then shaken for 10 s. After washing, adherent cells were fixed with 4% formaldehyde and stained with crystal violet (5 mg/ml in 2% ethanol) for 10 min. Cells were washed with water, dried and lysed with 2% SDS for 30 min. Adhesion was quantified measuring the absorption at 550 nm.

Western blotting

Cells were lysed in RIPA buffer containing proteinase inhibitor cocktail (Roche), 1 mM DTT, and 2 mM Na_3VO_4. Proteins were separated by electrophoresis on 10% polyacrylamide/SDS gels and transferred to OPTITRAN nitrocellulose filters (Whatman). Membranes were blocked with 5% skim milk or 5% bovine serum albumin in 0.05% Tween 20 in TBST and stained with primary antibodies at 4°C over night. The membrane was washed and incubated with peroxidase-conjugated secondary antibody (Dako) for 2 h at room temperature. Detection of chemiluminescence was done with the AceGlow substrate (Peqlab). Quantification of band intensities was performed with Gel-Pro Analyzer 6.0 (Media Cybernetics). The following primary antibodies were used: phospho-AKT (Ser473) (587F11, Cell Signaling), AKT (9272, Cell Signaling), ERK1/2 (K-23, Santa Cruz), phospho-ERK1/2 (E-4, Santa Cruz), SYNJ2BP (ab69431, Abcam), DLL4 (#2589, Cell Signaling), DLL1 (#2588, Cell Signaling), cleaved Notch1 (Val 1744, #2421, Cell Signaling), GAPDH (6C5, Abcam), VCP (T0307, Sigma-Aldrich), and phospho-SMAD2/3 (#8828, Cell Signaling).

Cycloheximide assay, DLL1 & DLL4 half-life determination

To assess DLL4 protein stability, HUAEC were transduced with GFP or SYNJ2BP adenovirus. To investigate DLL1 stability, HUAECs had to be additionally transduced with DLL1 lentivirus with MOI=2, as endogenous DLL1 expression was low. Furthermore, DLL1 stability was assessed in freshly prepared HUVEC (passage 0) in which DLL1 was high enough for detection. After 48 h the growth medium was replaced with medium containing 0.1 mM cycloheximide to halt protein biosynthesis. Cells were treated for 0-8 h and then harvested for Western blotting. For inhibition of the proteasome or the lysosome, 1 µM lactacystin, 300 µM chloroquine, respectively, was added to the medium 2 h before the onset of the cycloheximide treatment.

Co-immunoprecipitation

Control HUVEC and HUVEC transduced with SYNJ2BP and DLL4 adenovirus 48 h before were harvested with 300 µL IP buffer (140 mM NaCl, 5 mM EDTA, 20 mM HEPES, pH 7.5, 1% Nonidet P40 (Igepal), 1× Complete Protease Inhibitor Cocktail (Roche)) per 10 cm dish, incubated for 15 min on ice and disrupted with a cell scraper. The crude lysate was centrifuged at 4000 rpm for 15 min to remove cell debris. 25 µL pan-mouse antibody-coupled ferromagnetic beads (Dynabeads) were washed four times with 500 µL IP buffer, employing a magnetic rack for quick precipitation. 2 µg SYNJ2BP antibody (ab69431, Abcam) were added and incubated for 2 h at 4°C on a rotating wheel. To remove unbound antibody the beads were again washed four times. The lysate supernatant was applied to the beads, followed by incubation at 4°C on a rotating wheel over night. Again the beads where washed four times with IP buffer, precipitated proteins were released by heating the beads to 95°C with 4x Lämmli buffer for 3 min.

To assess DLL4 ubiquitinylation, HEK 293T cells were transfected with pLenti-hDLL4 and pRK5-HA-ubiquitin (#17608, Addgene) with or without pLenti-hSYNJ2BP. After 48 h, cells were harvested with 370 µl IP-buffer per 10 cm dish. Immunoprecipitation was performed with an antibody against the HA-probe (F-7, sc-7392, Santa Cruz).

Quantitative RT-PCR (qPCR)

Total RNA was isolated using the RNeasy Kit (Qiagen) and up to 5 µg RNA was transcribed into cDNA with SuperScript II Reverse Transcriptase and random hexamer primers (Invitrogen). 1 µl diluted cDNA was used for qPCR using the POWER SYBR Green Master Mix in a 25 µl reaction on an ABI StepOnePlus cycler (Applied Biosystems). Product sizes were controlled by evaluation of the melt curves using the ABI StepOnePlus cycler software. C_t-values were determined with LinReg software[8] and normalization was done with the housekeeping genes OAZ1, HPRT, GAPDH, and SRP14.[9] For the evaluation of the retinopathy of prematurity model, vWF and CD31 were used as housekeeping genes to take the different amounts of endothelial cells in the control samples and samples with increased angiogenesis into account. Primer sequences are listed in **suppl. Table I**.

LUMIER interaction assay

LUminescence-based Mammalian IntERactome mapping is an automated high-throughput technology designed for the systematic mapping of dynamic protein-protein interaction networks in mammalian cells[10] and was done in cooperation with the Genomics and Proteomics Core Facility, DKFZ Heidelberg. Expression constructs were designed by cloning the construct cDNA into the expression vectors pT-REx-DEST30-ctProteinA and pcDNA3-ntRenLuc-GW (Genomics and Proteomics Core Facility, DKFZ Heidelberg). Expression constructs in the Gateway vectors pT-REx-DEST30-ctProteinA and pcDNA3-ntRenLuc-GW were transiently transfected into HEK293 cells. After 48 h cells were lysed and protein A-tagged proteins were purified on immunoglobulin-coated magnetic beads. Luciferase activity was measured in the lysate before and after washing. As a negative control, the expression construct for the protein A-tagged protein was replaced by a construct of protein A only. As a positive control, the known protein-protein interaction JUN-FOS was measured in parallel. Luciferase activity was converted into z-scores as a measure of interaction. A z-score indicates how many standard deviations an observation or datum is above or below the mean. It is a dimensionless quantity derived by subtracting the population mean from an individual raw score and then dividing the difference by the population standard deviation. The values for mean and standard deviations have been approximated from large screening campaigns at the Genomics and Proteomics Core Facility, DKFZ Heidelberg.

Coculture and C2C12 cell differentiation

For coculture experiments with C2C12 cells, HUVEC adenovirally transduced with lacZ or SYNJ2BP for 24 h were seeded with half of the number of C2C12 at high density on gelatine-coated cover slips. Cells were cultured and differentiated in endothelial growth medium with SupplementMix (Pan Biotech) and 2.5% FCS (Biochrom). Cells were fixed and permeabilized after 24–48 h for 5 minutes at -20°C with methanol. Fast-twitch skeletal myosin heavy chains were detected using an anti-MHC (MY-32) antibody (1:500; Sigma) and an Alexa Fluor 546-coupled secondary antibody (Molecular Probes). Nuclei were stained with DAPI. Images were taken with a fluorescence microscope (Zeiss Axio Imager.Z1; AxioCam HRc camera). For the coculture experiments with mouse lung endothelial cells, HUVEC were transfected with siRNA

silencing DLL4 or SYNJ2BP. After 48 h, the HUVEC were mixed in a 1:2 ratio with the mLEC and cultured for 30 h. Following mRNA isolation the experiments were analysed with qPCR.

Determination of DLL1 endocytosis rate

DLL1 internalization was measured as described[11] with minor modifications. Immortalized HUVEC stably expressing DLL1 (inserted by lentiviral transduction) were transduced with adenovirus to induce expression of GFP or SYNJ2BP. After 48 h, cells were serum starved for 30 min, transferred to ice, washed twice in cold PBS, and surface labeled with 0.2 mg/ml NHS-SS-biotin (Pierce) in PBS for 30 min at 4°C. Labeled cells were washed in cold PBS and transferred to normal growth medium at 37°C in the presence of 0.06 µM primaquine to allow internalization without recycling. At 0, 5, and 10 min the medium was aspirated, and the dishes were rapidly transferred to ice and washed twice with ice-cold PBS. Biotin was removed from proteins remaining at the cell surface by incubation with a solution containing 20 mM MesNa in 50 mM Tris (pH 8.6) and 100 mM NaCl for 30 min at 4°C. The cells were lysed in 200 mM NaCl, 75 mM Tris, 15 mM NaF, 1.5 mM Na_3VO_4, 7.5 mM EDTA, 7.5 mM EGTA, 1.5% Triton X-100, 0.75% Igepal CA-630, and proteinase inhibitor cocktail (Roche Diagnostics). Lysates were clarified by centrifugation at 10,000 x g for 10 min. Levels of biotinylated DLL1 in the supernatants were determined by capture-ELISA employing plates coated with hDLL1-antibody (1F9) produced in rat, which was a gift from Dr. A. Gossler, University of Hannover, Germany. The amount of cell surface DLL1 was calculated by normalization of the levels of biotinylated DLL1 in samples with 0 min internalization time to the respective GAPDH levels measured by Western blotting.

Statistical analyses

Results are expressed as means plus/minus standard deviations unless stated otherwise. Comparisons between groups were analyzed by a 2-sided t-test. Probability values smaller 0.05 were considered significant.

References

1. Leimeister C, Dale K, Fischer A, Klamt B, Hrabe de Angelis M, Radtke F, McGrew MJ, Pourquie O, Gessler M. Oscillating expression of c-hey2 in the presomitic mesoderm suggests that the segmentation clock may use combinatorial signaling through multiple interacting bhlh factors. *Dev Biol*. 2000;227:91-103
2. Dong QG, Bernasconi S, Lostaglio S, De Calmanovici RW, Martin-Padura I, Breviario F, Garlanda C, Ramponi S, Mantovani A, Vecchi A. A general strategy for isolation of endothelial cells from murine tissues. Characterization of two endothelial cell lines from the murine lung and subcutaneous sponge implants. *Arterioscler Thromb Vasc Biol*. 1997;17:1599-1604
3. Hammes HP, Brownlee M, Jonczyk A, Sutter A, Preissner KT. Subcutaneous injection of a cyclic peptide antagonist of vitronectin receptor-type integrins inhibits retinal neovascularization. *Nat Med*. 1996;2:529-533
4. Brutsch R, Liebler SS, Wustehube J, Bartol A, Herberich SE, Adam MG, Telzerow A, Augustin HG, Fischer A. Integrin cytoplasmic domain-associated protein-1 attenuates sprouting angiogenesis. *Circ Res*. 2010;107:592-601
5. Alajati A, Laib AM, Weber H, Boos AM, Bartol A, Ikenberg K, Korff T, Zentgraf H, Obodozie C, Graeser R, Christian S, Finkenzeller G, Stark GB, Heroult M, Augustin HG.

Spheroid-based engineering of a human vasculature in mice. *Nat Methods*. 2008;5:439-445
6. Laib AM, Bartol A, Alajati A, Korff T, Weber H, Augustin HG. Spheroid-based human endothelial cell microvessel formation in vivo. *Nat Protoc*. 2009;4:1202-1215
7. Baker M, Robinson SD, Lechertier T, Barber PR, Tavora B, D'Amico G, Jones DT, Vojnovic B, Hodivala-Dilke K. Use of the mouse aortic ring assay to study angiogenesis. *Nat Protoc*. 2012;7:89-104
8. Ruijter JM, Ramakers C, Hoogaars WM, Karlen Y, Bakker O, van den Hoff MJ, Moorman AF. Amplification efficiency: Linking baseline and bias in the analysis of quantitative pcr data. *Nucleic Acids Res*. 2009;37:e45
9. de Jonge HJ, Fehrmann RS, de Bont ES, Hofstra RM, Gerbens F, Kamps WA, de Vries EG, van der Zee AG, te Meerman GJ, ter Elst A. Evidence based selection of housekeeping genes. *PLoS One*. 2007;2:e898
10. Barrios-Rodiles M, Brown KR, Ozdamar B, Bose R, Liu Z, Donovan RS, Shinjo F, Liu Y, Dembowy J, Taylor IW, Luga V, Przulj N, Robinson M, Suzuki H, Hayashizaki Y, Jurisica I, Wrana JL. High-throughput mapping of a dynamic signaling network in mammalian cells. *Science*. 2005;307:1621-1625
11. Roberts M, Barry S, Woods A, van der Sluijs P, Norman J. Pdgf-regulated rab4-dependent recycling of alphavbeta3 integrin from early endosomes is necessary for cell adhesion and spreading. *Curr Biol*. 2001;11:1392-1402

SUPPLEMENTARY DATA

suppl. Figure I

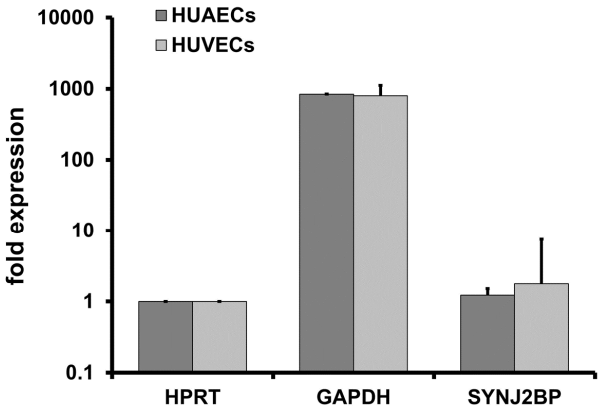

Suppl. Fig. I. Expression of SYNJ2BP in primary human endothelial cells. qPCR comparison of gene expression levels between HUVEC and HUAEC demonstrated that SYNJ2BP was expressed in both cell types at similar levels. Expression values were normalized to HPRT1 and the fold expression was calculated from the target gene ΔC_t values. GAPDH served as additional reference gene. n=3. Results are expressed as means plus standard deviation.

suppl. Figure II

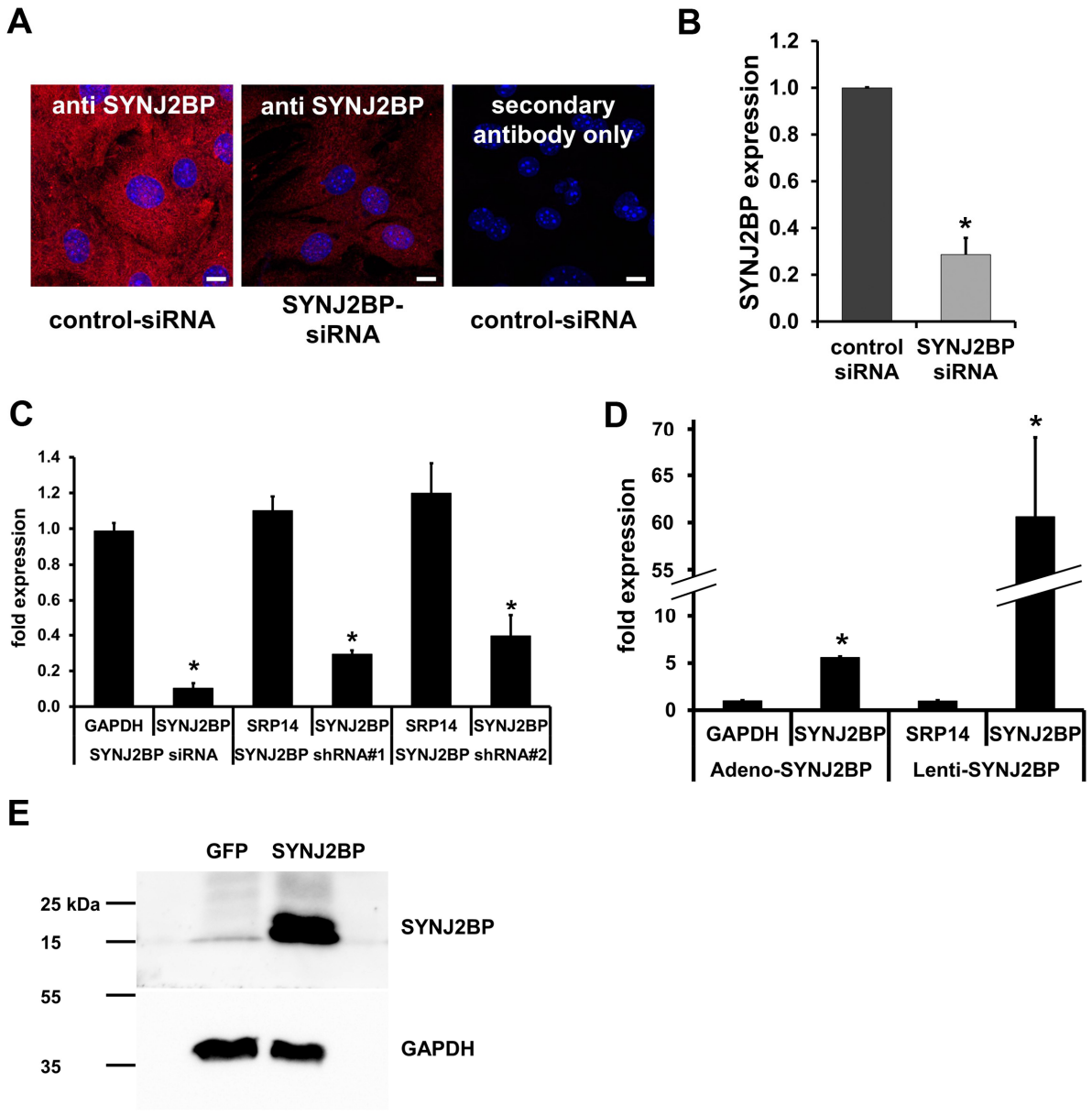

Suppl. Fig. II. Manipulation of SYNJ2BP in primary endothelial cells. (**A**) Immunofluorescence staining of murine lung endothelial cells with a SYNJ2BP antibody or with the secondary antibody only confirmed the effectivity of SYNJ2BP silencing and antibody specificity. Scale bar, 10 nm. (**B**) qPCR analysis of murine lung endothelial cells transfected with SYNJ2BP siRNA demonstrated effective SYNJ2BP silencing. n=2; results are expressed as means plus standard deviation. *, $p<0.05$. (**C**) qPCR showed that silencing of SYNJ2BP expression with siRNA and shRNA significantly reduced SYNJ2BP expression in HUVEC. Expression values were normalized to OAZ1 or HPRT1 and compared to HUVEC transfected with control-siRNA or transduced with non-silencing shRNA-lentivirus. GAPDH and SRP14 served as additional internal controls. n=3. (**D**) qPCR analysis of HUVEC transduced with SYNJ2BP adenovirus or

lentivirus. Both viruses induced a significant increase in SYNJ2BP expression. Expression values were normalized to OAZ1 or HPRT1 and compared to GFP expressing cells. GAPDH and SRP14 served as additional internal controls. n=3. Results are expressed as means plus standard deviation. *, p<0.05. (**E**) Western blot of HUVEC infected with GFP or SYNJ2BP lentivirus. Detection with a SYNJ2BP antibody confirmed an increase of SYNJ2BP protein expression 48 h after viral transduction.

suppl. Figure III

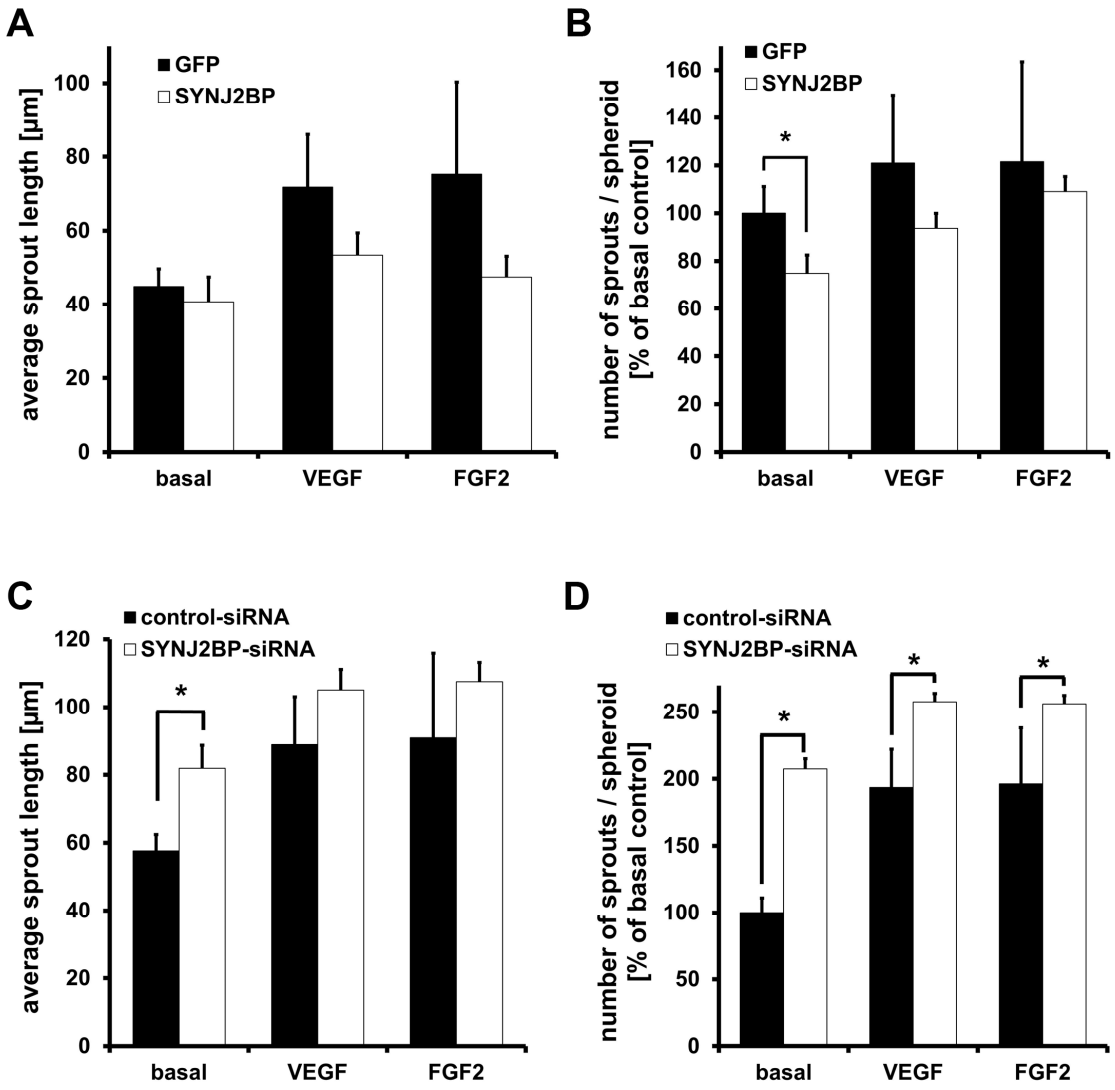

Suppl. Fig. III. Effects of SYNJ2BP on sprouting angiogenesis. (**A, B**) SYNJ2BP overexpression in HUVEC. The average sprout length and the average number of sprouts were reduced. n=4 independent assays. (**C,D**) siRNA-mediated silencing of SYNJ2BP expression. The average sprout length was increased under basal conditions. The sprout number was increased under all tested conditions suggesting that SYNJ2BP was required to suppress the tip cell

phenotype. n=5 independent assays. Results are expressed as means plus standard deviation. *, p<0.05.

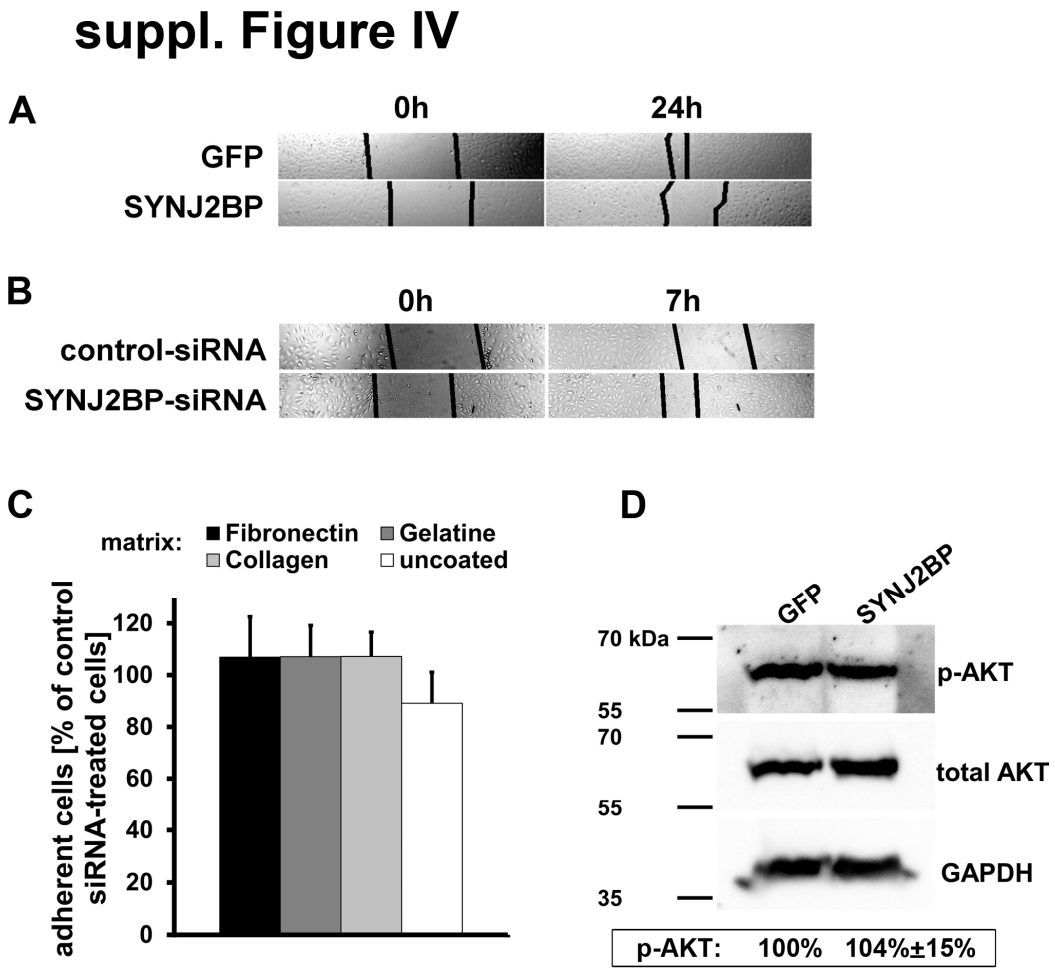

Suppl. Fig. IV. SYNJ2BP controls migration but not adhesion. (**A**) Representative images showing that forced SYNJ2BP expression led to decreased HUVEC migration in a wound healing assay. Images were taken using the phase-contrast microscope Olympus IX50 at 4-fold magnification. (**B**) SYNJ2BP-silencing resulted in a significant increase of endothelial cell migration compared to control-siRNA transduced HUVEC. (**C**) Adhesion to different extracellular matrix molecules was not significantly altered following SYNJ2BP silencing indicating that the increased migration upon SYNJ2BP silencing was not due to altered adhesion. n=4. Results are expressed as means plus standard deviation. (**D**) Western blot of HUVEC expressing SYNJ2BP or GFP showed that AKT phosphorylation was not significantly altered by SYNJ2BP. Area density quantification confirmed AKT phosphorylation levels of 104% ± 15% (n=3).

suppl. Figure V

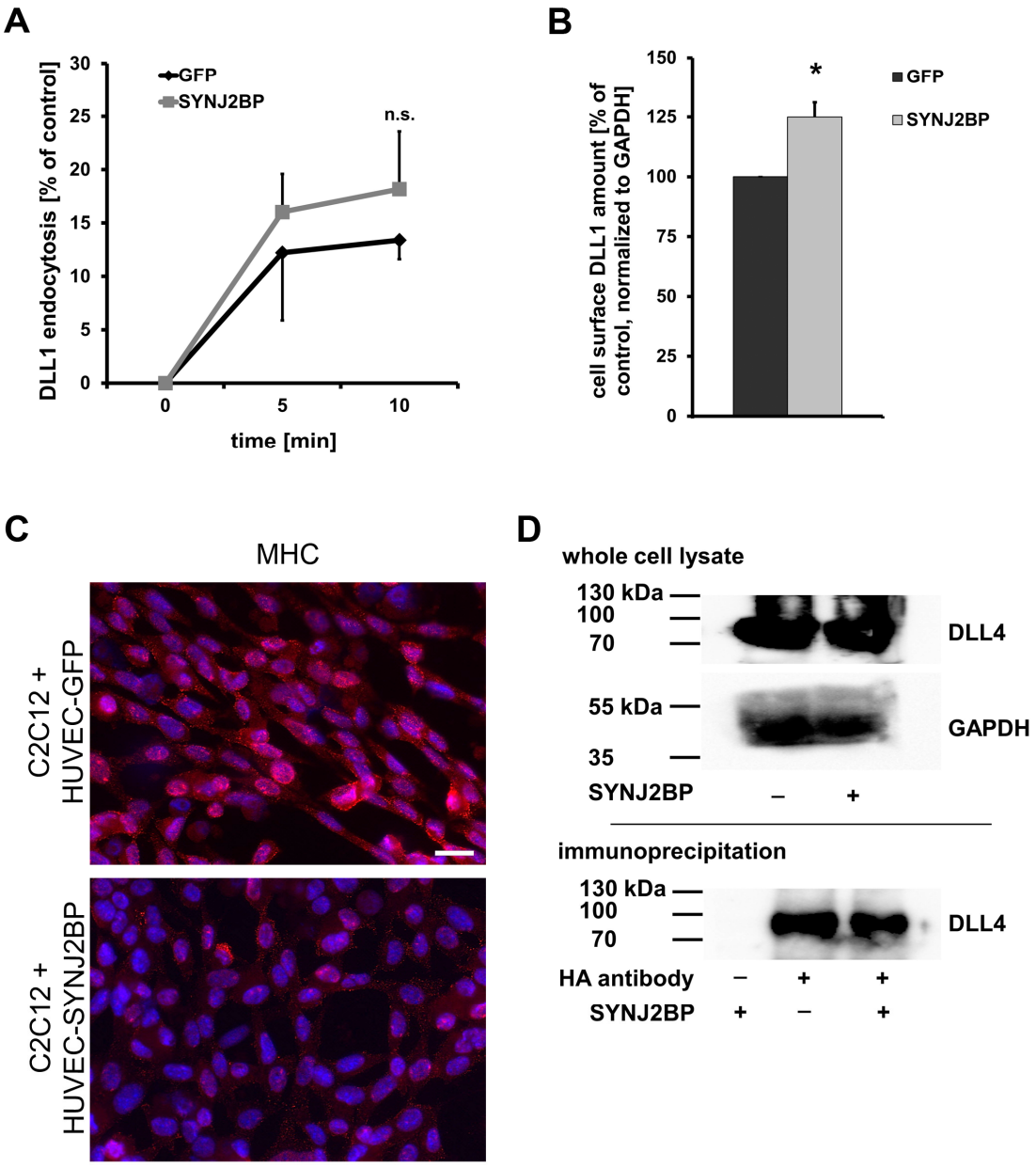

Suppl. Fig. V. SYNJ2BP enhances Notch signaling independent of DLL1 endocytosis and DLL4 ubiquitinylation. (A) Internalization rate of DLL1 after forced expression of SYNJ2BP or GFP. Immortalized HUVEC constitutively expressing DLL1 were surface-labeled with NHS-SS-biotin and incubated at 37°C for the indicated times. Proteins remaining at the cell surface were debiotinylated and the rate of internalized (still biotinylated) DLL1 was determined by ELISA. n=3, n.s., not significant. Results are expressed as means plus or minus standard error. (**B**) The amount of cell surface DLL1 was normalized to the total protein content (quantified by measuring GAPDH by Western blotting). Forced expression of SYNJ2BP increased the DLL1 cell surface

amount by 25%. n=3, results are expressed as means plus standard deviation. *, p<0.05. (**C**) C2C12 myoblast differentiation was inhibited by co-culture with SYNJ2BP-expressing HUVEC compared to GFP-expressing HUVEC. Fast skeletal myosin heavy chain expression (MHC, stained in red) indicated myoblast differentiation. Nuclei were stained with DAPI (blue). Images were taken with a fluorescence microscope (Zeiss Axio Imager.Z1; AxioCam HRc camera). Scale bar, 20 µm. (**D**) Western blots of the co-immunoprecipitation of DLL4 with ubiquitin-HA and the corresponding whole cell lysates for comparison. Normalization of the ubiquitinylated DLL4 (precipitated with an HA antibody) to the total DLL4 amount present in the cells revealed no significant difference in DLL4 ubiquitinylation with or without forced SYNJ2BP expression. n=2.

suppl. Figure VI

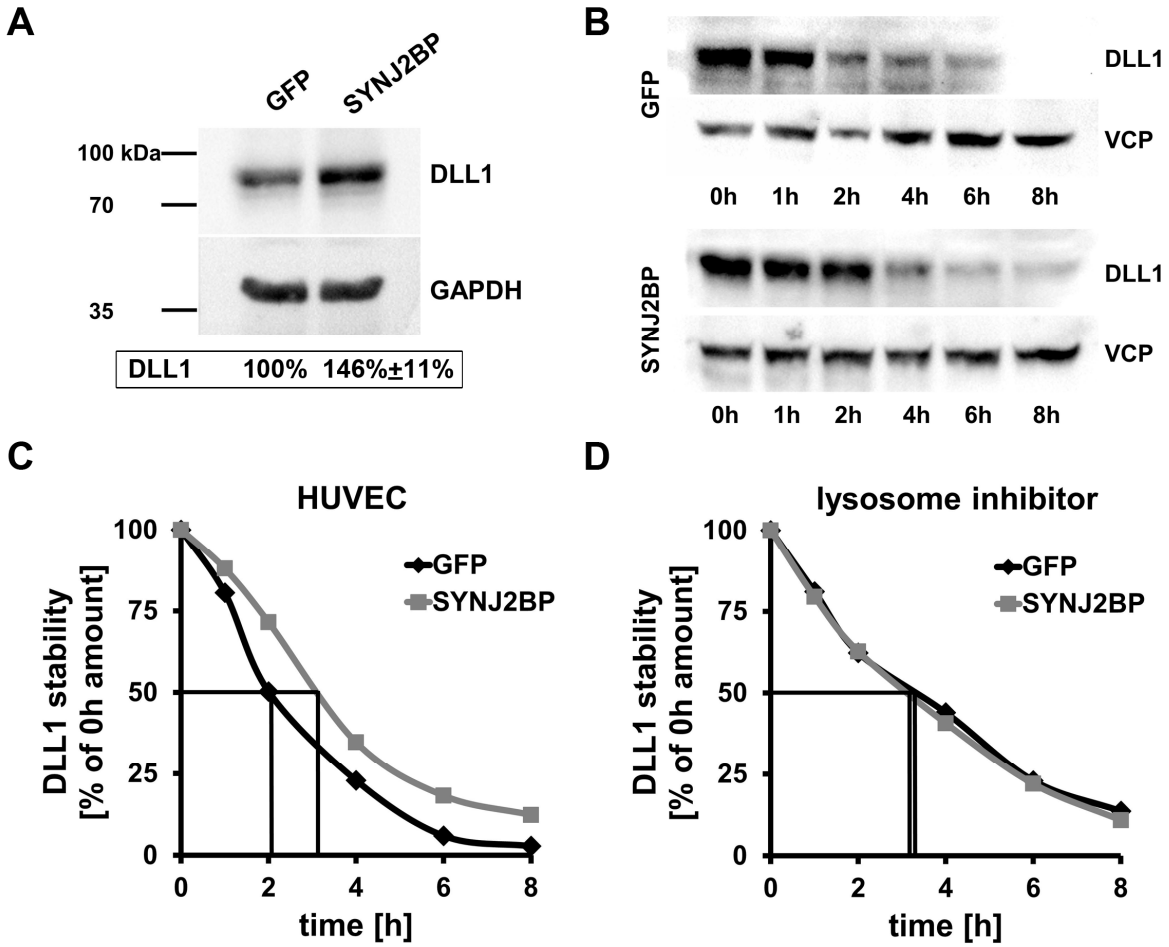

Suppl. Fig. VI. SYNJ2BP promotes endothelial DLL1 stability. (A) Western blotting after SYNJ2BP gain-of-function in lentivirally transduced (MOI=2) HUAEC revealed increased DLL1 proteins levels compared to GFP control (146% ± 11%). GAPDH was used as loading control. n=2. (**B**) 48 h after viral infection HUAEC were cultured in the presence of 0.1 mM cycloheximide to block protein synthesis (time point 0 h). Western blotting of protein lysates at different time

points showed increased stability of DLL1 protein. (**C**) HUVEC were adenovirally transduced to express SYNJ2BP or GFP. After 48 h the cells were treated with cycloheximide for 0 – 8 h. Quantification of Western blot bands revealed an increased DLL1 protein half-life of from 130 to 190 min when SYNJ2BP was expressed. (**D**) In presence of the lysosome inhibitor chloroquine (300 µM), DLL1 half-life in HUAEC was 190 min with and 200 min without SYNJ2BP overexpression.

suppl. Figure VII

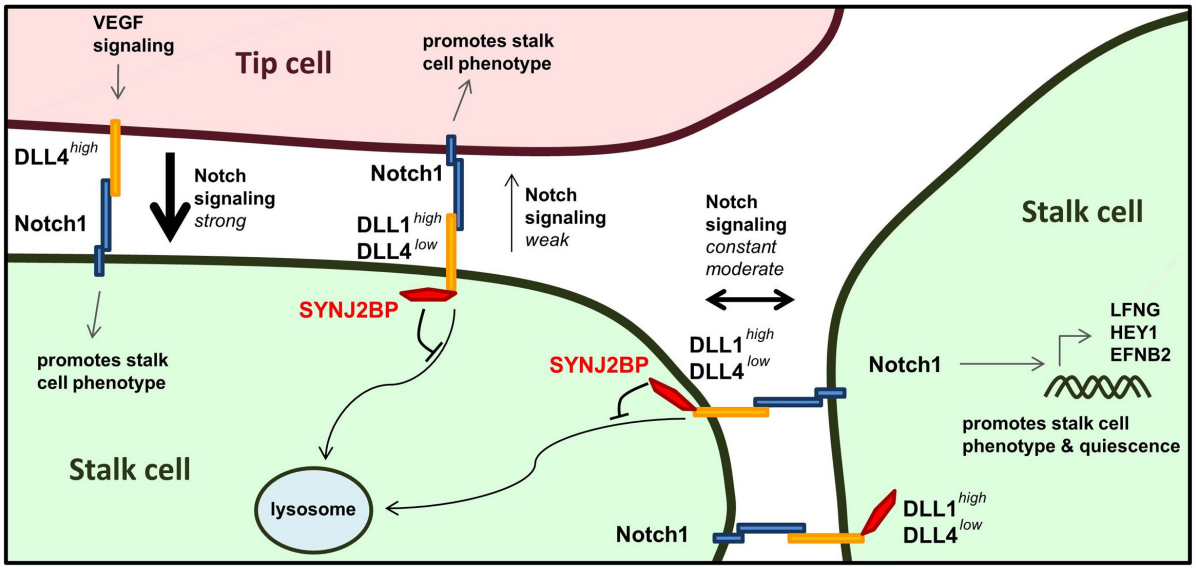

Suppl. Fig. VII. Schematic diagram summarizing the role of SYNJ2BP in Delta-Notch signaling during angiogenesis. SYNJ2BP is expressed in stalk cells where it binds to and stabilizes the Notch ligands DLL1 and DLL4. This induces Notch signalling in the neighboring cells, promoting the stalk cell phenotype. The constant moderate levels of Notch signaling in the stalk cell plexus are necessary for vessel remodeling and preventing excessive vessel branching.

suppl. Table I

gene name	location and direction	sequence
hANGPT2	exon 7 forward	GGGAAGGGAATGAGGCTTAC
	exon 9 reverse	AAGTTGGAAGGACCACATGC
hApelin	exon 2 forward	CCCAGAGGGTCAAGGAATG
	exon 2 reverse	AGAAAGGCATGGGTCCCTTA
mCD31	exon 6 forward	AGAGACGGTCTTGTCGCAGT
	exon 7 reverse	TACTGGGCTTCGAGAGCATT
mDLL1ic (-BamHI)	exon 9 forward	cacGGATCCcggctgaagctacagaaaca
	3'UTR reverse	cacGGATCCttacacctcagtcgctataac
mDLL1	exon 8 forward	ACTGCAGCTCTTCACCCTGT
	exon 9 reverse	CAGGTGCAGGAGAAGTCGTT
mDLL4	exon 9 forward	AGAAGGTGCCACTTCGGTTA
	3'UTR reverse	AGCTGGGTGTCTGAGTAGGC
mDLL4ic (-BamHI)	exon 9 forward	cacGGATCCcggcagctgcggcttcggag
	3'UTR reverse	cacGGATCCttatacctctgtggcaatcac
mDLL1ic (-PDZ-BamHI)	exon 10 reverse	cacGGATCCTTAtataacacactcatccttttctg
mDLL4ic (-PDZ-BamHI)	exon 10 reverse	cacGGATCCTTAgaagagaggaacgagtgtgtgat
hEFNB2	exon 4 forward	CTGCTGGATCAACCAGGAAT
	exon 5 reverse	GATGTTGTTCCCCGAATGTC
hESM1	exon 1 forward	CTTGCTACCGCACAGTCTCA
	exon 2 reverse	ACTGGCAGTTGCAGGTCTCT
hGAPDH	exon 7 forward	TGCACCACCAACTGCTTAGC
	exon 8 reverse	TTCAGCTCAGGGATGACCTT
mGAPDH	exon 4 forward	AACTTTGGCATTGTGGAAGG
	exon 5 reverse	ACACATTGGGGGTAGGAACA
hHEY1	exon 3 forward	GAGAAGGCTGGTACCCAGTG
	exon 5 reverse	CGAAATCCCAAACTCCGATA
mHEY1	exon 2/3 forward	GAAAAGACGGAGAGGCATCA
	exon 4/5 reverse	GTGCGCGTCAAAATAACCTT
mHEY2	exon 2 forward	AGGTCCAATTCACCGACAAC
	exon 5 reverse	AGCATGGGCATCAAAGTAGC

hHPRT1	exon 3 forward	GTCAAGGGCATATCCTACAACAA
	exon 5 reverse	AAGATGGTCAAGGTCGCAAG
mHPRT1	exon 8 forward	TGTTGTTGGATATGCCCTTG
	exon 9 reverse	ACTGGCAACATCAACAGGACT
hLFNG	exon 3 forward	AGATGGCCGTGGAGTATGAC
	exon 4/5 reverse	GACAGGACGcACCTTGTTCT
hNOTCH1	exon 33 forward	CTGAAGAACGGGGCTAACAA
	exon 34 reverse	CAGGTTGTACTCGTCCAGCA
hOAZ1	exon 4 forward	GAGCCGACCATGTCTTCATT
	exon 5 reverse	CTCCTCCTCTCCCGAAGACT
hSRP14	exon 4 forward	AGGGTACTGTGGAGGGCTTT
	exon 6 reverse	GCTGTTGTTGCTGCTGTTGT
hSYNJ2BP	exon 3 forward	CTGCACCAGGATGCTGTAGA
	exon 4 reverse	TGGCACCAGCACCATAAATA
mSYNJ2BP	exon 2 forward	TCCAACGACAGTGGCATCTA
	exon 3 reverse	TCTCAGGGACACAGCACATC
mSYNJ2BP (-BamHI)	exon 1 forward	gcgggatccatgAACGGACGGGTGGATTATT
mSYNJ2BP (-EcoRI)	3'UTR reverse	gcggaattcGGAAGACAGCAAGCATTtca
hVEGF-C	exon 1 forward	TTGCTGGGCTTCTTCTCTGT
	exon 2 reverse	TGCTCCTCCAGATCTTTGCT
mvWF	exon 4 forward	GGCAAGAGAATGAGCCTGTC
	exon 5 reverse	AAGCCAAAGGTCTCACTGGA